Structural Engineering and Mechanics, *Vol. 53, No. 3 (2015) 537-573*
DOI: http://dx.doi.org/10.12989/sem.2015.53.3.537

Differential transform method and numerical assembly technique for free vibration analysis of the axial-loaded Timoshenko multiple-step beam carrying a number of intermediate lumped masses and rotary inertias

Yusuf Yesilce*

Department of Civil Engineering, Dokuz Eylul University, 35160, Buca, Izmir, Turkey

(Received August 28, 2014, Revised November 11, 2014, Accepted November 25, 2014)

Abstract. Multiple-step beams carrying intermediate lumped masses with/without rotary inertias are widely used in engineering applications, but in the literature for free vibration analysis of such structural systems; Bernoulli-Euler Beam Theory (BEBT) without axial force effect is used. The literature regarding the free vibration analysis of Bernoulli-Euler single-span beams carrying a number of spring-mass systems, Bernoulli-Euler multiple-step and multi-span beams carrying multiple spring-mass systems and multiple point masses are plenty, but that of Timoshenko multiple-step beams carrying intermediate lumped masses and/or rotary inertias with axial force effect is fewer. The purpose of this paper is to utilize Numerical Assembly Technique (NAT) and Differential Transform Method (DTM) to determine the exact natural frequencies and mode shapes of the axial-loaded Timoshenko multiple-step beam carrying a number of intermediate lumped masses and/or rotary inertias. The model allows analyzing the influence of the shear and axial force effects, intermediate lumped masses and rotary inertias on the free vibration analysis of the multiple-step beams by using Timoshenko Beam Theory (TBT). At first, the coefficient matrices for the intermediate lumped mass with rotary inertia, the step change in cross-section, left-end support and right-end support of the multiple-step Timoshenko beam are derived from the analytical solution. After the derivation of the coefficient matrices, NAT is used to establish the overall coefficient matrix for the whole vibrating system. Finally, equating the overall coefficient matrix to zero one determines the natural frequencies of the vibrating system and substituting the corresponding values of integration constants into the related eigenfunctions one determines the associated mode shapes. After the analytical solution, an efficient and easy mathematical technique called DTM is used to solve the differential equations of the motion. The calculated natural frequencies of Timoshenko multiple-step beam carrying intermediate lumped masses and/or rotary inertias for the different values of axial force are given in tables. The first five mode shapes are presented in graphs. The effects of axial force, intermediate lumped masses and rotary inertias on the free vibration analysis of Timoshenko multiple-step beam are investigated.

Keywords: differential transform method; free vibration; intermediate lumped mass with/without rotary inertia; natural frequency; numerical assembly technique; Timoshenko multiple-step beam

*Corresponding author, Associate Professor, E-mail: yusuf.yesilce@deu.edu.tr

http://www.techno-press.org/?journal=sem&subpage=8 ISSN: 1225-4568 (Print), 1598-6217 (Online)

1. Introduction

Beams with step changes in cross-section occur in civil and mechanical engineering structural elements. The free vibration characteristics of a uniform or non-uniform beam carrying various concentrated elements (such as intermediate point masses, rotary inertias, linear springs, rotational springs, etc.) is an important problem in engineering. Thus, a lot of studies have been published in this area.

The normal mode summation technique to determine the fundamental frequency of the cantilever beams carrying masses and springs was used by Gürgöze (1984, 1985). Hamdan and Jubran (1991) investigated the free and forced vibrations of a restrained uniform beam carrying an intermediate lumped mass and a rotary inertia. Ju *et al.* (1994) investigated the free vibration analysis of arbitrarily stepped beams by using the first-order shear deformation theory and finite element method. Gürgöze *et al.* solved the eigenfrequencies of a cantilever beam with attached tip mass and a spring-mass system and studied the effect of an attached spring-mass system on the frequency spectrum of a cantilever beam (Gürgöze *et al.* 1996, Gürgöze 1996, 1998). Moreover, they studied on two alternative formulations of the frequency equation of a Bernoulli-Euler beam to which several spring-mass systems being attached in-span and then solved for the eigenfrequencies. Liu *et al.* (1998) formulated the frequency equation for beams carrying intermediate concentrated masses by using the Laplace Transformation Technique. Wu and Chou (1999) obtained the exact solution of the natural frequency values and mode shapes for a beam carrying any number of spring masses. The free vibration analysis of a uniform Timoshenko beam carrying multiple spring-mass systems was studied by Wu and Chen (2001). Gürgöze and Erol (2001, 2002) investigated the forced vibration responses of a cantilever beam with single intermediate support. Naguleswaran (2002a, b) investigated the natural frequencies and mode shapes of a Bernoulli-Euler beam with one-step and three-step changes in cross-sections. Chen and Wu (2002) obtained the exact natural frequencies and mode shapes of the non-uniform beams with multiple spring-mass systems. Naguleswaran (2002c, 2003a) obtained the natural frequency values of the beams on up to five resilient supports including ends and carrying several particles by using BEBT and a fourth-order determinant equated to zero. Chen (2003) investigated the natural frequencies and mode shapes of the non-uniform beams carrying multiple various concentrated elements. The vibration and stability of an axial-loaded Bernoulli-Euler beams with step changes in cross-sections and carrying a non-symmetrical rigid body at the step were investigated by Naguleswaran (2003b, 2004a, b). Lin and Chang (2005) studied the free vibration analysis of a multi-span Timoshenko beam with an arbitrary number of flexible constraints by considering the compatibility requirements on each constraint point and using a transfer matrix method. Lin and Tsai (2005, 2006, 2007) determined the exact natural frequencies and mode shapes for Bernoulli-Euler multi-span beam carrying multiple point masses, a number of intermediate lumped masses and rotary inertias and multiple spring-mass systems. Koplow *et al*. (2006) studied the closed form solutions for the dynamic analysis of Bernoulli-Euler beams with step changes in cross-sections. Wang *et al*. (2007) studied the natural frequencies and mode shapes of a uniform Timoshenko beam carrying multiple intermediate spring-mass systems with the effects of shear deformation and rotary inertia. In the other study, the flexural-free vibration of a cantilevered beam with multiple cross-section steps is investigated theoretically and experimentally by Jaworski and Dowell (2008). Yesilce *et al.* (2008) investigated the effects of attached spring-mass systems on the free vibration characteristics of the 1-4 span Timoshenko beams. In the other studies, Yesilce *et al.* investigated the natural frequencies of vibration of Timoshenko and Reddy-Bickford multi-span beams carrying multiple spring-mass systems with axial force effect (Yesilce and Demirdag 2008, Yesilce 2010). Lin (2008) investigated the free and forced vibration characteristics of Bernoulli-Euler multi-span beam carrying a number of various concentrated elements. Lin (2010) investigated the free vibration characteristics of non-uniform Bernoulli-Euler beam carrying multiple elastic-supported rigid bars. Wu and Chang (2013) investigated the exact solution for free vibration of a non-uniform beam carrying any number of concentrated elements including lumped mass with rotary inertias and spring mass systems is presented by using the continuous-mass transfer matrix method.

DTM was applied to solve linear and non-linear initial value problems and partial differential equations by many researches. The concept of DTM was first introduced by Zhou (1986) and he used DTM to solve both linear and non-linear initial value problems in electric circuit analysis. Özdemir and Kaya (2006) investigated flapwise bending vibration analysis of a rotating tapered cantilever Bernoulli-Euler beam by DTM. In the other studies, the out-of-plane free vibration analysis of a double tapered Bernoulli-Euler beam and a rotating, double tapered Timoshenko beam featuring coupling between flapwise bending and torsional vibrations are performed using DTM by Ozgumus and Kaya (2006, 2007). Çatal (2006, 2008, 2012) suggested DTM for the free vibration analysis of Timoshenko beams resting on elastic soil foundation and forced vibration analysis of Bernoulli-Euler beams. Çatal and Çatal (2006) calculated the critical buckling loads of partially embedded Timoshenko pile in elastic soil by DTM. In the other study, Kaya and Ozgumus (2007) introduced DTM to analyze the free vibration response of an axially loaded, closed-section composite Timoshenko beam which features material coupling between flapwise bending and torsional vibrations due to ply orientation. For the first time, Yesilce and Catal (2009) investigated the free vibration analysis of one fixed, the other end simply supported Reddy-Bickford beam by using DTM in the other study. Since previous studies have shown DTM to be an efficient tool and it has been applied to solve boundary value problems for many linear, non-linear integro-differential and differential-difference equations that are very important in fluid mechanics, viscoelasticity, control theory, acoustics, etc.

In the presented paper, we describe the determination of the natural frequencies and mode shapes of the axial-loaded Timoshenko multiple-step beam carrying a number of intermediate lumped masses and rotary inertias by using NAT and DTM. The natural frequencies of the beams are calculated, the first five mode shapes are plotted and the effects of the axial force and the influence of the shear are investigated by using the computer package, Matlab. Unfortunately, a suitable example that studies the free vibration analysis of Timoshenko multiple-step beam carrying intermediate lumped masses and/or rotary inertias with axial force effect using NAT and DTM has not been investigated by any of the studies in open literature so far.

2. The mathematical model and formulation

An axial-loaded Timoshenko beam with h-step changes in cross-sections and carrying n intermediate lumped masses and s rotary inertias is presented in Fig. 1. From Fig. 1, the total number of intermediate stations is $M'=h+n+s-f$ with f denoting the total number of overlapped stations for step changes in cross-sections, lumped masses and/or rotary inertias. The kinds of coordinates which are used in this study are given below:

$x_{v'}$ are the position vectors for the stations,)$1\leq v'\leq M'+2$,

x_p^* are the position vectors of the intermediate lumped masses, ($1\leq p\leq n$),

$\bar{x}_r$ are the position vectors of the step changes in cross-sections, ($1 \le r \le h$),
$\hat{x}_j$ are the position vectors of the rotary inertias, ($1 \le j \le s$).

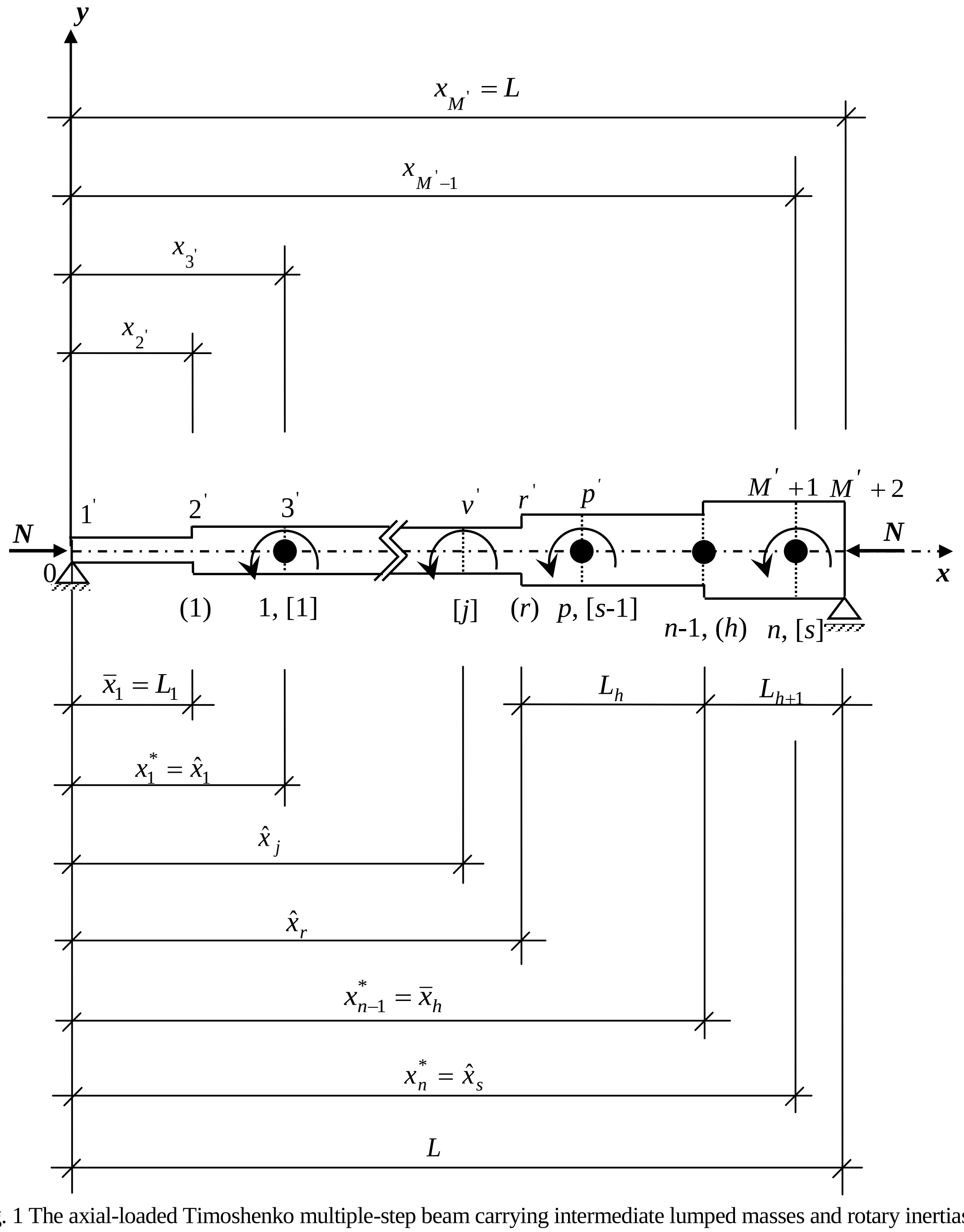

Fig. 1 The axial-loaded Timoshenko multiple-step beam carrying intermediate lumped masses and rotary inertias

From Fig. 1, the symbols of 1′, 2′,..., *v*′,..., *M*′+1, *M*′+2 above the *x*-axis refer to the numbering of stations. The symbols of 1, 2, ..., *p*, ...,*n* below the *x*-axis refer to the numbering of the intermediate lumped masses. The symbols of (1), (2), ..., (*r*), ..., (*h*) below the *x*-axis refer to the numbering of the step changes in cross-sections. The symbols of [1], [2], ..., [*j*], ..., [*s*] below the *x*-axis refer to the numbering of the rotary inertias.

Using Hamilton's principle, the equations of motion for the axial-loaded Timoshenko multiple-step beam can be written as

$$EI_i \cdot \frac{\partial^2 \phi_i(x_i,t)}{\partial x_i^2} + \frac{GA_i \cdot}{\bar{k}} \cdot \left(\frac{\partial y_i(x_i,t)}{\partial x_i} - \phi_i(x_i,t) \right) - \frac{\overline{m}_i \cdot I_i}{A_i} \cdot \frac{\partial^2 \phi_i(x_i,t)}{\partial t^2} = 0 \quad (1.a)$$

$$\frac{GA_i \cdot}{\bar{k}} \cdot \left(\frac{\partial^2 y_i(x_i,t)}{\partial x_i^2} - \frac{\partial \phi_i(x_i,t)}{\partial x_i} \right) - N \cdot \frac{\partial^2 y_i(x_i,t)}{\partial x_i^2} - \overline{m}_i \cdot \frac{\partial^2 y_i(x_i,t)}{\partial t^2} = 0$$

$$(0 \le x_i \le L_i) \quad (i = 1, 2, ..., h+1) \quad (1.b)$$

where $y_i(x_i,t)$ represents transverse deflection of the i^{th} beam segment; $\phi_i(x_i,t)$ is the rotation angle due to bending moment of the i^{th} beam segment; $\overline{m}_i$ is mass per unit length of the i^{th} beam segment; N is the axial compressive force; A_i is the cross-section area of the i^{th} beam segment; I_i is moment of inertia of the i^{th} beam segment; L_i is the length of the i^{th} beam segment; $\bar{k}$ is the shape factor due to cross-section geometry of the beam; E, G are Young's modulus and shear modulus of the beam, respectively; x_i is the position of the i^{th} beam segment; t is time variable. The details for the application of Hamilton's principle and the derivation of the equations of motion are presented in Appendix at the end of the paper.

The parameters appearing in the foregoing expressions have the following relationships:

$$\frac{\partial y_i(x_i,t)}{\partial x_i} = \phi_i(x_i,t) + \gamma_i(x_i,t) \quad (2.a)$$

$$M_i(x_i,t) = EI_i \cdot \frac{\partial \phi_i(x_i,t)}{\partial x_i} \quad (2.b)$$

$$T_i(x_i,t) = \frac{GA_i}{\bar{k}} \cdot \gamma_i(x_i,t) = \frac{GA_i}{\bar{k}} \cdot \left(\frac{\partial y_i(x_i,t)}{\partial x_i} - \phi_i(x_i,t) \right) \quad (2.c)$$

where $M_i(x_i,t)$ and $T_i(x_i,t)$ are the bending moment function and shear force function of the i^{th} beam segment, respectively, and $\gamma_i(x_i,t)$ is the associated shearing deformation of the i^{th} beam segment.

After some manipulations by using Eqs. (1) and (2), one obtains the following uncoupled equations of motion for the axial-loaded Timoshenko multiple-step beam as

$$\left(1 - \frac{N \cdot \bar{k}}{GA_i}\right) \cdot EI_i \cdot \frac{\partial^4 y_i(x_i,t)}{\partial x_i^4} + N \cdot \frac{\partial^2 y_i(x_i,t)}{\partial x_i^2} + \overline{m}_i \cdot \frac{\partial^2 y_i(x_i,t)}{\partial t^2}$$

$$- \left(1 + \frac{E \cdot \bar{k}}{G} - \frac{N \cdot \bar{k}}{GA_i}\right) \cdot \frac{\partial^4 y_i(x_i,t)}{\partial x_i^2 \cdot \partial t^2} + \frac{\overline{m}_i^2 \cdot I_i \cdot \bar{k}}{A_i^2 \cdot G} \cdot \frac{\partial^4 y_i(x_i,t)}{\partial t^4} = 0 \quad (3.a)$$

$$\left(1-\frac{N\cdot\bar{k}}{GA_i}\right)\cdot EI_i\cdot\frac{\partial^4\phi_i(x_i,t)}{\partial x_i^4}+N\cdot\frac{\partial^2\phi_i(x_i,t)}{\partial x_i^2}+\bar{m}_i\cdot\frac{\partial^2\phi_i(x_i,t)}{\partial t^2}$$
$$-\left(1+\frac{E\cdot\bar{k}}{G}-\frac{N\cdot\bar{k}}{GA_i}\right)\cdot\frac{\partial^4\phi_i(x_i,t)}{\partial x_i^2\cdot\partial t^2}+\frac{\bar{m}_i^2\cdot I_i\cdot\bar{k}}{A_i^2\cdot G}\cdot\frac{\partial^4\phi_i(x_i,t)}{\partial t^4}=0 \tag{3.b}$$

The general solution of Eq. (3) can be obtained by using the method of separation of variables as

$$y_i(x_i,t)=y_i(x_i)\cdot\sin(\omega\cdot t) \tag{4.a}$$

$$\phi_i(x_i,t)=\phi_i(x_i)\cdot\sin(\omega\cdot t)\qquad \left(0\le z_i\le L_i/L\right)\left(i=1,2,...,h+1\right) \tag{4.b}$$

in which

$$y_i(z_i)=\left[C_{i,1}.\cosh(D_{i,1}.z_i)+C_{i,2}.\sinh(D_{i,1}.z_i)+C_{i,3}.\cos(D_{i,2}.z_i)+C_{i,4}.\sin(D_{i,2}.z_i)\right]$$

$$\phi_i(z_i)=\left[K_{i,3}\cdot C_{i,1}.\sinh(D_{i,1}.z_i)+K_{i,3}\cdot C_{i,2}.\cosh(D_{i,1}.z_i)+K_{i,4}\cdot C_{i,3}.\sin(D_{i,2}.z_i)-K_{i,4}\cdot C_{i,4}.\cos(D_{i,2}.z_i)\right]$$

$$D_{i,1}=\sqrt{\frac{1}{2}\cdot\left(-\beta_i+\sqrt{\beta_i^2+4\cdot\alpha_i^4}\right)};\quad D_{i,2}=\sqrt{\frac{1}{2}\cdot\left(\beta_i+\sqrt{\beta_i^2+4\cdot\alpha_i^4}\right)};$$

$N_r=\dfrac{N\cdot L^2}{EI_1}$ (nondimensionalized multiplication factor for the axial compressive force of the first beam segment);

$\lambda_i=\sqrt[4]{\dfrac{\bar{m}_i.\omega^2.L^4}{EI_i}}$ (frequency factor for the *i*th beam segment);

$$\alpha_i^4=\frac{\lambda_i^4\cdot EI_i-\dfrac{\bar{m}_i^2\cdot I_i\cdot\bar{k}\cdot\omega^4\cdot L^4}{A_i^2\cdot G}}{\left(1-\dfrac{N_r\cdot EI_1\cdot\bar{k}}{GA_i\cdot L^2}\right)\cdot EI_i};\ \beta_i=\frac{\left[\dfrac{N_r\cdot EI_1}{L^2}+\left(1+\dfrac{E\cdot\bar{k}}{GA_i}-\dfrac{N_r\cdot EI_1\cdot\bar{k}}{GA_i\cdot L^2}\right)\cdot\dfrac{\bar{m}_i\cdot I_i}{A_i}\cdot\omega^2\right]\cdot L^2}{\left(1-\dfrac{N_r\cdot EI_1\cdot\bar{k}}{GA_i\cdot L^2}\right)\cdot EI_i};$$

$$K_{i,3}=\frac{GA_i\cdot D_{i,1}}{\bar{k}\cdot\left(-EI_i\cdot D_{i,1}^2-\dfrac{\bar{m}_i\cdot I_i}{A_i}\cdot\omega^2+\dfrac{GA_i}{\bar{k}}\right)};\quad K_{i,4}=\frac{-GA_i\cdot D_{i,2}}{\bar{k}\cdot\left(EI_i\cdot D_{i,2}^2-\dfrac{\bar{m}_i\cdot I_i}{A_i}\cdot\omega^2+\dfrac{GA_i}{\bar{k}}\right)}$$

$z_i=\dfrac{x_i}{L}$; $C_{i,1}$, ..., $C_{i,4}$ are the constants of integration; L is total length of the beam; ω is the natural circular frequency of the vibrating system.

The bending moment and shear force functions of the *i*th beam segment with respect to z_i are given below

$$M_i(z_i,t)=\frac{EI_i}{L}\cdot\frac{d\phi_i(z_i)}{dz_i}\cdot\sin(\omega\cdot t) \tag{5.a}$$

$$T_i(z_i, t) = \frac{GA_i}{\bar{k}} \cdot \left(\frac{1}{L} \cdot \frac{dy_i(z_i)}{dz_i} - \phi_i(z_i) \right) \cdot \sin(\omega \cdot t) \quad (i = 1, 2, ..., h+1) \tag{5.b}$$

3. Determination of the natural frequencies and mode shapes

The state is written due to the values of the displacement, slope, bending moment and shear force functions at the locations of z_i and t for the i^{th} segment of Timoshenko beam, as

$$\{S_i(z_i, t)\}^T = \{y_i(z_i) \quad \phi_i(z_i) \quad M_i(z_i) \quad T_i(z_i)\} \cdot \sin(\omega . t) \tag{6}$$

where $\{S_i(z_i,t)\}$ shows the state vector of the i^{th} beam segment.

If the left-end support of the beam is pinned (as shown in Fig. 1), the boundary conditions for the left-end support are written as

$$y_{1'}(z = 0) = 0 \tag{7.a}$$

$$M_{1'}(z = 0) = 0 \tag{7.b}$$

From Eqs. (2) and (3), the boundary conditions for the left-end pinned support can be written in matrix equation form as

$$[B_{1'}] \cdot \{C_{1'}\} = \{0\} \tag{8.a}$$

$$\begin{array}{cc} \begin{matrix} 1 & \quad 2 & \quad 3 & \quad 4 \end{matrix} & \\ \begin{bmatrix} 1 & 0 & 1 & 0 \\ K_{1,1} & 0 & -K_{1,2} & 0 \end{bmatrix} & \begin{matrix} 1 \\ 2 \end{matrix} \end{array} \cdot \begin{Bmatrix} C_{1',1} \\ C_{1',2} \\ C_{1',3} \\ C_{1',4} \end{Bmatrix} = \begin{Bmatrix} 0 \\ 0 \end{Bmatrix} \tag{8.b}$$

where $K_{1,1} = \dfrac{EI_1 \cdot K_{1,3} \cdot D_{1,1}}{L}$; $K_{1,2} = -\dfrac{EI_1 \cdot K_{1,4} \cdot D_{1,2}}{L}$

In the formula of $K_{1,1}$ and $K_{1,2}$, 1 denotes the 1^{st} beam segment.

If the left-end support of the beam is clamped, the boundary conditions are written as

$$y_{1'}(z = 0) = 0 \tag{9.a}$$

$$\phi_{1'}(z = 0) = 0 \tag{9.b}$$

From Eqs. (2) and (5), the boundary conditions for the left-end clamped support can be written in matrix equation form as

$$\begin{array}{cc} \begin{matrix} 1 & \quad 2 & \quad 3 & \quad 4 \end{matrix} & \\ \begin{bmatrix} 1 & 0 & 1 & 0 \\ 0 & K_{1,3} & 0 & -K_{1,4} \end{bmatrix} & \begin{matrix} 1 \\ 2 \end{matrix} \end{array} \cdot \begin{Bmatrix} C_{1',1} \\ C_{1',2} \\ C_{1',3} \\ C_{1',4} \end{Bmatrix} = \begin{Bmatrix} 0 \\ 0 \end{Bmatrix} \tag{10}$$

If the left-end support of the beam is free, the boundary conditions are written as

$$M_{1'}\left(z=0\right)=0 \tag{11.a}$$

$$T_{1'}\left(z=0\right)=0 \tag{11.b}$$

From Eqs. (3) and (4), the boundary conditions for the free left-end can be written in matrix equation form as

$$\begin{array}{cccc} 1 & 2 & 3 & 4 \end{array}$$
$$\begin{array}{c}\begin{bmatrix} K_{1,1} & 0 & -K_{1,2} & 0 \\ 0 & K_{1,5} & 0 & -K_{1,6} \end{bmatrix}\end{array}\begin{array}{c}1\\2\end{array} \cdot \begin{Bmatrix} C_{1',1} \\ C_{1',2} \\ C_{1',3} \\ C_{1',4} \end{Bmatrix} = \begin{Bmatrix} 0 \\ 0 \end{Bmatrix} \tag{12}$$

where $K_{1,5}=\dfrac{GA_1}{\bar{k}}\cdot\left(\dfrac{D_{1,1}}{L}-K_{1,3}\right)$; $K_{1,6}=\dfrac{GA_1}{\bar{k}}\cdot\left(-\dfrac{D_{1,2}}{L}-K_{1,4}\right)$

In the formula of $K_{1,5}$ and $K_{1,6}$, 1 denotes the 1^{st} beam segment.

The boundary conditions for the p^{th} intermediate lumped mass with rotary inertia in the i^{th} beam segment are written by using continuity of deformations, slopes and equilibrium of bending moments and shear forces, as (the station numbering corresponding to the p^{th} intermediate lumped mass is represented by p')

$$y_{p'}^{L}\left(z_{p'}\right)=y_{p'}^{R}\left(z_{p'}\right) \tag{13.a}$$

$$\phi_{p'}^{L}\left(z_{p'}\right)=\phi_{p'}^{R}\left(z_{p'}\right) \tag{13.b}$$

$$M_{p'}^{L}\left(z_{p'}\right)+I_{0,p}\cdot\omega^2\cdot\phi_{p'}^{L}\left(z_{p'}\right)=M_{p'}^{R}\left(z_{p'}\right) \tag{13.c}$$

$$T_{p'}^{L}\left(z_{p'}\right)+m_p\cdot\omega^2\cdot y_{p'}^{L}\left(z_{p'}\right)=T_{p'}^{R}\left(z_{p'}\right) \tag{13.d}$$

where m_p is the magnitude of the lumped mass; $I_{0,p}$ is the rotary inertia; L and R refer to the left side and right side of the p^{th} intermediate lumped mass, respectively.

The boundary conditions for the p^{th} intermediate lumped mass with rotary inertia in the i^{th} beam segment are presented in matrix equation form as

$$\left[B_{p'}\right]\cdot\left\{C_{p'}\right\}=\left\{0\right\} \tag{14}$$

where

$$\left\{C_{p'}\right\}^T=\left\{C_{p'-1,1}\quad C_{p'-1,2}\quad C_{p'-1,3}\quad C_{p'-1,4}\quad C_{p',1}\quad C_{p',2}\quad C_{p',3}\quad C_{p',4}\right\} \tag{15.a}$$

$$\left[B_{p'}\right]=\begin{array}{c} \\ \\ \\ \\ \\ \end{array}\begin{array}{cccccccc} 4p'-3 & 4p'-2 & 4p'-1 & 4p' & 4p'+1 & 4p'+2 & 4p'+3 & 4p'+4 \\ \end{array}$$

$$\left[B_{p'}\right]=\begin{bmatrix} ch_{i,1} & sh_{i,1} & cs_{i,2} & sn_{i,2} & -ch_{i,1} & -sh_{i,1} & -cs_{i,2} & -sn_{i,2} \\ K_{i,3}\cdot sh_{i,1} & K_{i,3}\cdot ch_{i,1} & K_{i,4}\cdot sn_{i,2} & -K_{i,4}\cdot cs_{i,2} & -K_{i,3}\cdot sh_{i,1} & -K_{i,3}\cdot ch_{i,1} & -K_{i,4}\cdot sn_{i,2} & K_{i,4}\cdot cs_{i,2} \\ K_{i,7} & K_{i,8} & K_{i,9} & K_{i,10} & -K_{i,1}\cdot ch_{i,1} & -K_{i,1}\cdot sh_{i,1} & K_{i,2}\cdot cs_{i,2} & K_{i,2}\cdot sn_{i,2} \\ K_{i,11} & K_{i,12} & K_{i,13} & K_{i,14} & -K_{i,5}\cdot sh_{i,1} & -K_{i,5}\cdot ch_{i,1} & -K_{i,6}\cdot sn_{i,2} & K_{i,6}\cdot cs_{i,2} \end{bmatrix}\begin{array}{c} 4p'-1 \\ 4p' \\ 4p'+1 \\ 4p'+2 \end{array} \tag{15.b}$$

where

$$ch_{i,1}=\cosh\left(D_{i,1}\cdot z_{p'}\right);\ sh_{i,1}=\sinh\left(D_{i,1}\cdot z_{p'}\right);\ cs_{i,2}=\cos\left(D_{i,2}\cdot z_{p'}\right);\ sn_{i,2}=\sin\left(D_{i,2}\cdot z_{p'}\right)$$

$$K_{i,7}=K_{i,1}\cdot ch_{i,1}-K_{i,3}\cdot I_{0,p}\cdot\omega^2\cdot sh_{i,1}\ ;\quad K_{i,8}=K_{i,1}\cdot sh_{i,1}-K_{i,3}\cdot I_{0,p}\cdot\omega^2\cdot ch_{i,1}$$

$$K_{i,9}=-K_{i,2}\cdot cs_{i,2}-K_{i,4}\cdot I_{0,p}\cdot\omega^2\cdot sn_{i,2}\ ;\ K_{i,10}=-K_{i,2}\cdot sn_{i,2}+K_{i,4}\cdot I_{0,p}\cdot\omega^2\cdot cs_{i,2}$$

$$K_{i,11}=K_{i,5}\cdot sh_{i,1}+m_p\cdot\omega^2\cdot ch_{i,1}\ ;\ K_{i,12}=K_{i,5}\cdot ch_{i,1}+m_p\cdot\omega^2\cdot sh_{i,1}$$

$$K_{i,13}=K_{i,6}\cdot sn_{i,2}+m_p\cdot\omega^2\cdot cs_{i,2}\ ;\ K_{i,14}=-K_{i,6}\cdot cs_{i,2}+m_p\cdot\omega^2\cdot sn_{i,2}$$

In Eq. (13), $I_{0,p}$ is taken as 0.00 for the situation of the intermediate lumped mass without rotary inertia. In the same equation, $m_{,p}$ is taken as zero for the situation of rotary inertia without intermediate lumped mass. For this case, p is changed by j in Eqs. (13), (14) and (15).

The boundary conditions for the r^{th} step change in cross-section are written by using continuity of deformations, slopes and equilibrium of bending moments, as (the station numbering corresponding to the r^{th} step change in cross-section is represented by r')

$$y_{r'}^{L}\left(z_{r'}\right)=y_{r'}^{R}\left(z_{r'}\right) \tag{16.a}$$

$$\phi_{r'}^{L}\left(z_{r'}\right)=\phi_{r'}^{R}\left(z_{r'}\right) \tag{16.b}$$

$$M_{r'}^{L}\left(z_{r'}\right)=M_{r'}^{R}\left(z_{r'}\right) \tag{16.c}$$

$$T_{r'}^{L}\left(z_{r'}\right)=T_{r'}^{R}\left(z_{r'}\right) \tag{16.d}$$

The boundary conditions for the r^{th} step change in cross-section are presented in matrix equation form as

$$\left[B_{r'}\right]\cdot\left\{C_{r'}\right\}=\left\{0\right\} \tag{17}$$

where

$$\left\{C_{r'}\right\}^T=\left\{C_{r'-1,1}\quad C_{r'-1,2}\quad C_{r'-1,3}\quad C_{r'-1,4}\quad C_{r',1}\quad C_{r',2}\quad C_{r',3}\quad C_{r',4}\right\} \tag{18.a}$$

$$
\begin{array}{c}
\left[B_{r'}\right] = \\
\end{array}
\begin{array}{ccccc}
4r'-3 & 4r'-2 & 4r'-1 & 4r' & 4r'+1 \\
\end{array}
$$

$$
\left[B_{r'}\right]=\left[\begin{array}{ccccc}
chr_{i,1} & shr_{i,1} & csr_{i,2} & snr_{i,2} & chr_{i+1,1} \\
K_{i,3}\cdot shr_{i,1} & K_{i,3}\cdot chr_{i,1} & K_{i,4}\cdot snr_{i,2} & -K_{i,4}\cdot csr_{i,2} & -K_{i+1,3}\cdot shr_{i+1,1} \\
K_{i,1}\cdot chr_{i,1} & K_{i,1}\cdot shr_{i,1} & -K_{i,2}\cdot csr_{i,2} & -K_{i,2}\cdot snr_{i,2} & -K_{i+1,1}\cdot chr_{i+1,1} \\
K_{i,5}\cdot shr_{i,1} & K_{i,5}\cdot chr_{i,1} & K_{i,6}\cdot snr_{i,2} & -K_{i,6}\cdot csr_{i,2} & -K_{i+1,5}\cdot shr_{i+1,1}
\end{array}\right.
$$

$$
\begin{array}{c}
\begin{array}{ccc}
4r'+2 & 4r'+3 & 4r'+4
\end{array} \\
\left.\begin{array}{ccc}
shr_{i+1,1} & csr_{i+1,2} & snr_{i+1,2} \\
-K_{i+1,3}\cdot chr_{i+1,1} & -K_{i+1,4}\cdot snr_{i+1,2} & K_{i+1,4}\cdot csr_{i+1,2} \\
-K_{i+1,1}\cdot shr_{i+1,1} & K_{i+1,2}\cdot csr_{i+1,2} & K_{i+1,2}\cdot snr_{i+1,2} \\
-K_{i+1,5}\cdot chr_{i+1,1} & -K_{i+1,6}\cdot snr_{i+1,2} & K_{i+1,6}\cdot csr_{i+1,2}
\end{array}\right]
\begin{array}{c}
4r'-1 \\ 4r' \\ 4r'+1 \\ 4r'+2
\end{array}
\end{array}
\tag{18.b}
$$

where

$$chr_{i,1}=\cosh\left(D_{i,1}\cdot z_{r'}\right)\ ;\ shr_{i,1}=\sinh\left(D_{i,1}\cdot z_{r'}\right)\ ;\ csr_{i,2}=\cos\left(D_{i,2}\cdot z_{r'}\right)\ ;$$

$$snr_{i,2}=\sin\left(D_{i,2}\cdot z_{r'}\right)$$

$$chr_{i+1,1}=\cosh\left(D_{i+1,1}\cdot z_{r'}\right)\ ;\ shr_{i+1,1}=\sinh\left(D_{i+1,1}\cdot z_{r'}\right)\ ;\ csr_{i+1,2}=\cos\left(D_{i+1,2}\cdot z_{r'}\right)\ ;$$

$$snr_{i+1,2}=\sin\left(D_{i+1,2}\cdot z_{r'}\right)$$

If the right-end support of the beam is pinned, the boundary conditions for the right-end support are written as

$$y_{M'}(z=1)=0 \tag{19.a}$$

$$M_{M'}(z=1)=0 \tag{19.b}$$

From Eqs. (2) and (3), the boundary conditions for the right-end pinned support can be written in matrix equation form as

$$\left[B_{M'}\right]\cdot\left\{C_{M'}\right\}=\{0\} \tag{20}$$

where

$$\left\{C_{M'}\right\}^{T}=\left\{C_{M',1}\quad C_{M',2}\quad C_{M',3}\quad C_{M',4}\right\} \tag{21.a}$$

$$
\begin{array}{c}
\begin{array}{cccc}
4M'+1 & 4M'+2 & 4M'+3 & 4M'+4
\end{array} \\
\left[B_{M'}\right]=\left[\begin{array}{cccc}
\cosh\left(D_{k+1,1}\right) & \sinh\left(D_{k+1,1}\right) & \cos\left(D_{k+1,2}\right) & \sin\left(D_{k+1,2}\right) \\
K_{k+1,1}\cdot\cosh\left(D_{k+1,1}\right) & K_{k+1,1}\cdot\sinh\left(D_{k+1,1}\right) & -K_{k+1,2}\cdot\cos\left(D_{k+1,2}\right) & -K_{k+1,2}\cdot\sin\left(D_{k+1,2}\right)
\end{array}\right]
\begin{array}{c} q-1 \\ q \end{array}
\end{array}
\tag{21.b}
$$

If the right-end support of the beam is clamped, the boundary conditions for the right-end support are written as

$$y_{M'}(z=1)=0 \tag{22.a}$$

$$\phi_{M'}(z=1)=0 \tag{22.b}$$

From Eqs. (2) and (5), the boundary coefficient matrix for the right-end support can be written as

$$\begin{array}{cccccc} & 4M'+1 & 4M'+2 & 4M'+3 & 4M'+4 & \\ [B_{M'}]= & \left[\begin{matrix} \cosh(D_{k+1,1}) \\ K_{k+1,3}\cdot\sinh(D_{k+1,1}) \end{matrix}\right. & \begin{matrix} \sinh(D_{k+1,1}) \\ K_{k+1,3}\cdot\cosh(D_{k+1,1}) \end{matrix} & \begin{matrix} \cos(D_{k+1,2}) \\ K_{k+1,4}\cdot\sin(D_{k+1,2}) \end{matrix} & \left.\begin{matrix} \sin(D_{k+1,2}) \\ -K_{k+1,4}\cdot\cos(D_{k+1,2}) \end{matrix}\right] & \begin{matrix} q-1 \\ q \end{matrix} \end{array} \tag{23}$$

If the right-end support of the beam is free, the boundary conditions are written as

$$M_{M'}(z=1)=0 \tag{24.a}$$

$$T_{M'}(z=1)=0 \tag{24.b}$$

From Eqs. (3) and (4), the boundary coefficient matrix for the free right-end can be written as

$$\begin{array}{cccccc} & 4M'+1 & 4M'+2 & 4M'+3 & 4M'+4 & \\ [B_{M'}]= & \left[\begin{matrix} K_{k+1,1}\cdot\cosh(D_{k+1,1}) \\ K_{k+1,5}\cdot\sinh(D_{k+1,1}) \end{matrix}\right. & \begin{matrix} K_{k+1,1}\cdot\sinh(D_{k+1,1}) \\ K_{k+1,5}\cdot\cosh(D_{k+1,1}) \end{matrix} & \begin{matrix} -K_{k+1,2}\cdot\cos(D_{k+1,2}) \\ K_{k+1,6}\cdot\sin(D_{k+1,2}) \end{matrix} & \left.\begin{matrix} -K_{k+1,2}\cdot\sin(D_{k+1,2}) \\ -K_{k+1,6}\cdot\cos(D_{k+1,2}) \end{matrix}\right] & \begin{matrix} q-1 \\ q \end{matrix} \end{array} \tag{25}$$

where

$$M'=h+n+s-f \tag{26}$$

In Eq. (26), $M'$is the total number of intermediate stations.

In Eqs. (21.b), (23) and (25), q denotes the total number of equations for integration constants given by

$$q=2+4\cdot M'+2 \tag{27}$$

From Eq. (27), it can be seen that; the left-end support of the beam has two equations, each intermediate station of the beam has four equations and the right-end support of the beam has two equations.

In this study, the coefficient matrices for left-end support, each intermediate lumped mass with/without rotary inertia and right-end support of the axial-loaded Timoshenko multiple-step beam are derived, respectively. In the next step, the numerical assembly technique is used to establish the overall coefficient matrix for the whole vibrating system as is given in Eq.(28). In the last step, for non-trivial solution, equating the last overall coefficient matrix to zero one determines the natural frequencies of the vibrating system as is given in Eq.(29) and substituting of the last integration constants into the related eigenfunctions one determines the associated mode shapes.

$$[B] \cdot \{C\} = \{0\} \tag{28}$$

$$|B| = 0 \tag{29}$$

4. The differential transform method (DTM)

Partial differential equations are often used to describe engineering problems whose closed form solutions are very difficult to establish in many cases. Therefore, approximate numerical methods are often preferred. However, in spite of the advantages of these on hand methods and the computer codes that are based on them, closed form solutions are more attractive due to their implementation of the physics of the problem and their convenience for parametric studies. Moreover, closed form solutions have the capability and facility to solve inverse problem of determining and designing the geometry and characteristics of an engineering system and to achieve a prescribed behavior of the system. Considering the advantages of the closed form solutions mentioned above, DTM is introduced in this study as the solution method (Yesilce and Catal 2009).

DTM is a semi-analytic transformation technique based on Taylor series expansion and is a useful tool to obtain analytical solutions of the differential equations. Certain transformation rules are applied and the governing differential equations and the boundary conditions of the system are transformed into a set of algebraic equations in terms of the differential transforms of the original functions in DTM. The solution of these algebraic equations gives the desired solution of the problem. The different from high-order Taylor series method is; Taylor series method requires symbolic computation of the necessary derivatives of the data functions and is expensive for large orders. DTM is an iterative procedure to obtain analytic Taylor series solutions of differential equations (Yesilce and Catal 2009).

A function $y(z)$, which is analytic in a domain D, can be represented by a power series with a center at $z=z_0$, any point in D. The differential transform of the function $y(z)$ is given by

$$Y(k) = \frac{1}{k!} \cdot \left(\frac{d^k y(z)}{dz^k} \right)_{z=z_0} \tag{30}$$

where $y(z)$ is the original function and $Y(k)$ is the transformed function. The inverse transformation is defined as

$$y(z) = \sum_{k=0}^{\infty} (z - z_0)^k \cdot Y(k) \tag{31}$$

From Eqs. (30) and (31) we get

$$y(z) = \sum_{k=0}^{\infty} \frac{(z - z_0)^k}{k!} \cdot \left(\frac{d^k y(z)}{dz^k} \right)_{z=z_0} \tag{32}$$

Eq. (32) implies that the concept of the differential transformation is derived from Taylor's series expansion, but the method does not evaluate the derivatives symbolically. However, relative derivative are calculated by iterative procedure that are described by the transformed equations of

Table 1 DTM theorems used for equations of motion

Original Function	Transformed Function
$y(z)=u(z)\pm v(z)$	$Y(k)=U(k)\pm V(k)$
$y(z)=a\cdot u(z)$	$Y(k)=a\cdot U(k)$
$y(z)=\dfrac{d^m u(z)}{dz^m}$	$Y(k)=\dfrac{(k+m)!}{k!}\cdot U(k+m)$
$y(z)=u(z)\cdot v(z)$	$Y(k)=\sum_{r=0}^{k} U(r)\cdot V(k-r)$
$y(z)=z^m$	$Y(k)=\delta(k-m)=\begin{cases}0 & \text{if } k\neq m\\ 1 & \text{if } k=m\end{cases}$

Table 2 DTM theorems used for boundary conditions

z=0		*z*=1	
Original Boundary Conditions	Transformed Boundary Conditions	Original Boundary Conditions	Transformed Boundary Conditions
$y(0)=0$	$Y(0)=0$	$y(1)=0$	$\sum_{k=0}^{\infty} Y(k)=0$
$\dfrac{dy}{dz}(0)=0$	$Y(1)=0$	$\dfrac{dy}{dz}(1)=0$	$\sum_{k=0}^{\infty} k\cdot Y(k)=0$
$\dfrac{d^2y}{dz^2}(0)=0$	$Y(2)=0$	$\dfrac{d^2y}{dz^2}(1)=0$	$\sum_{k=0}^{\infty} k\cdot(k-1)\cdot Y(k)=0$
$\dfrac{d^3y}{dz^3}(0)=0$	$Y(3)=0$	$\dfrac{d^3y}{dz^3}(1)=0$	$\sum_{k=0}^{\infty} k\cdot(k-1)\cdot(k-2)\cdot Y(k)=0$

the original functions. In real applications, the function *y*(*z*) in Eq. (31) is expressed by a finite series and can be written as

$$y(z)=\sum_{k=0}^{\bar{N}}(z-z_0)^k\cdot Y(k) \tag{33}$$

Eq. (10) implies that $\sum_{k=\bar{N}+1}^{\infty}(z-z_0)^k\, Y(k)$ is negligibly small. Where $\overline{N}$ is series size and the value of $\overline{N}$ depends on the convergence of the eigenvalues.

Theorems that are frequently used in differential transformation of the differential equations and the boundary conditions are introduced in Table 1 and Table 2, respectively.

4.1 Using differential transformation to solve motion equations

Eqs. (1.a) and (1.b) can be rewritten by using the method of separation of variables as follows

$$\frac{d^2\phi_i(z_i)}{dz_i^2} = -\left(\frac{GA_i \cdot L}{EI_i \cdot \bar{k}}\right)\cdot\frac{dy_i(z_i)}{dz_i} + \left(\frac{GA_i \cdot L^2}{EI_i \cdot \bar{k}} - \frac{\lambda_i^4 \cdot I_i}{A_i \cdot L^2}\right)\cdot \phi_i(z_i) \tag{34.a}$$

$$\frac{d^2 y_i(z_i)}{dz_i^2} = \left(\frac{GA_i \cdot L^3}{GA_i \cdot L^2 - N_r \cdot EI_1 \cdot \bar{k}}\right)\cdot\frac{d\phi_i(z_i)}{dz_i} - \left(\frac{\lambda_i^4 \cdot EI_i \cdot \bar{k}}{GA_i \cdot L^2 - N_r \cdot EI_1 \cdot \bar{k}}\right)\cdot y_i(z_i)$$

$$(0 \le z_i \le L_i/L) \qquad (i = 1, 2, ..., h+1) \tag{34.b}$$

The differential transform method is applied to Eqs. (34.a) and (34.b) by using the theorems introduced in Table 1 and the following expression are obtained

$$\Phi_i(k+2) = -\frac{1}{(k+2)}\cdot\left(\frac{GA_i \cdot L}{EI_i \cdot \bar{k}}\right)\cdot Y_i(k+1) + \frac{1}{(k+1)\cdot(k+2)}\cdot\left(\frac{GA_i \cdot L^2}{EI_i \cdot \bar{k}} - \frac{\lambda_i^4 \cdot I_i}{A_i \cdot L^2}\right)\cdot \Phi_i(k) \tag{35.a}$$

$$Y_i(k+2) = \frac{1}{(k+2)}\cdot\left(\frac{GA_i \cdot L^3}{GA_i \cdot L^2 - N_r \cdot EI_1 \cdot \bar{k}}\right)\cdot \Phi_i(k+1) - \frac{1}{(k+1)\cdot(k+2)}\cdot\left(\frac{\lambda_i^4 \cdot EI_i \cdot \bar{k}}{GA_i \cdot L^2 - N_r \cdot EI_1 \cdot \bar{k}}\right)\cdot Y_i(k) \tag{35.b}$$

where $Y_i(k)$ and $\Phi_i(k)$ are the transformed functions of $y_i(z_i)$ and $\phi_i(z_i)$, respectively.

The differential transform method is applied to Eqs. (5.a) and (5.b) by using the theorems introduced in Table 1 and the following expression are obtained

$$\overline{M}_i(k) = (k+1)\cdot\left(\frac{EI_i}{L}\right)\cdot \Phi_i(k+1) \tag{36.a}$$

$$\overline{T}_i(k) = \frac{GA_i}{\bar{k}}\cdot\left(\frac{k+1}{L}\cdot Y_i(k+1) - \Phi_i(k)\right) \tag{36.b}$$

where $\overline{M}_i(k)$ and $\overline{T}_i(k)$ are the transformed functions of $M_i(z_i)$ and $T_i(z_i)$, respectively.

If the left-end support of the beam is pinned; applying DTM to Eqs. (7.a) and (7.b), the transformed boundary conditions for the left-end support are written as

$$Y_{1'}(0) = \Phi_{1'}(1) = 0 \tag{37}$$

If the left-end support of the beam is clamped; applying DTM to Eqs. (9.a) and (9.b), the transformed boundary conditions for the left-end support are written as

$$Y_{1'}(0) = \Phi_{1'}(0) = 0 \tag{38}$$

If the left-end support of the beam is free; applying DTM to Eqs. (11.a) and (11.b), the transformed boundary conditions for the left-end support are written as

$$\Phi_{1'}(0) = \frac{Y_{1'}(1)}{L} \tag{39.a}$$

$$\Phi_{1'}(1) = 0 \tag{39.b}$$

The boundary conditions and the transformed boundary conditions of the p^{th} intermediate lumped mass with rotary inertia and the r^{th} step change in cross-section by applying the differential transform method, using the theorems introduced in Table 2 are presented in Table 3.

If the right-end support of the beam is pinned; applying DTM to Eqs. (19.a) and (19.b), the transformed boundary conditions for the right-end support are written as

$$\sum_{k=0}^{\bar{N}} Y_{M'}(k) = 0 \tag{40.a}$$

$$\sum_{k=0}^{\bar{N}} \overline{M}_{M'}(k) = 0 \tag{40.b}$$

If the right-end support of the beam is clamped; applying DTM to Eqs. (22.a) and (22.b), the transformed boundary conditions for the right-end support are written as

Table 3 The boundary conditions and the transformed boundary conditions of the p^{th} intermediate lumped mass with rotary inertia and the r^{th} step change in cross-section

Boundary Conditions	Transformed Boundary Conditions
$y_{p'}^{L}(z_{p'}) = y_{p'}^{R}(z_{p'})$	$\sum_{k=0}^{\bar{N}} z_{p'}^{k} \cdot Y_{p'}^{L}(k) - \sum_{k=0}^{\bar{N}} z_{p'}^{k} \cdot Y_{p'}^{R}(k) = 0$
$\phi_{p'}^{L}(z_{p'}) = \phi_{p'}^{R}(z_{p'})$	$\sum_{k=0}^{\bar{N}} z_{p'}^{k} \cdot \Phi_{p'}^{L}(k) - \sum_{k=0}^{\bar{N}} z_{p'}^{k} \cdot \Phi_{p'}^{R}(k) = 0$
$M_{p'}^{L}(z_{p'}) + I_{0,p} \cdot \omega^2 \cdot \phi_{p'}^{L}(z_{p'}) = M_{p'}^{R}(z_{p'})$	$\sum_{k=0}^{\bar{N}} z_{p'}^{k} \cdot \overline{M}_{p'}^{L}(k) + I_{0,p} \cdot \omega^2 \cdot \sum_{k=0}^{\bar{N}} z_{p'}^{k} \cdot \Phi_{p'}^{L}(k) - \sum_{k=0}^{\bar{N}} z_{p'}^{k} \cdot \overline{M}_{p'}^{R}(k) = 0$
$T_{p'}^{L}(z_{p'}) + m_p \cdot \omega^2 \cdot y_{p'}^{L}(z_{p'}) = T_{p'}^{R}(z_{p'})$	$\sum_{k=0}^{\bar{N}} z_{p'}^{k} \cdot \overline{T}_{p'}^{L}(k) + m_p \cdot \omega^2 \cdot \sum_{k=0}^{\bar{N}} z_{p'}^{k} \cdot Y_{p'}^{L}(k) - \sum_{k=0}^{\bar{N}} z_{p'}^{k} \cdot \overline{T}_{p'}^{R}(k) = 0$
$y_{r'}^{L}(z_{r'}) = y_{r'}^{R}(z_{r'})$	$\sum_{k=0}^{\bar{N}} z_{r'}^{k} \cdot Y_{r'}^{L}(k) - \sum_{k=0}^{\bar{N}} z_{r'}^{k} \cdot Y_{r'}^{R}(k) = 0$
$\phi_{r'}^{L}(z_{r'}) = \phi_{r'}^{R}(z_{r'})$	$\sum_{k=0}^{\bar{N}} z_{r'}^{k} \cdot \Phi_{r'}^{L}(k) - \sum_{k=0}^{\bar{N}} z_{r'}^{k} \cdot \Phi_{r'}^{R}(k) = 0$
$M_{r'}^{L}(z_{r'}) = M_{r'}^{R}(z_{r'})$	$\sum_{k=0}^{\bar{N}} z_{r'}^{k} \cdot \overline{M}_{r'}^{L}(k) - \sum_{k=0}^{\bar{N}} z_{r'}^{k} \cdot \overline{M}_{r'}^{R}(k) = 0$
$T_{r'}^{L}(z_{r'}) = T_{r'}^{R}(z_{r'})$	$\sum_{k=0}^{\bar{N}} z_{r'}^{k} \cdot \overline{T}_{r'}^{L}(k) - \sum_{k=0}^{\bar{N}} z_{r'}^{k} \cdot \overline{T}_{r'}^{R}(k) = 0$

$$\sum_{k=0}^{\bar{N}} Y_{M'}(k) = 0 \tag{41.a}$$

$$\sum_{k=0}^{\bar{N}} \Phi_{M'}(k) = 0 \tag{41.b}$$

If the right-end support of the beam is free; applying DTM to Eqs. (24.a) and (24.b), the transformed boundary conditions for the right-end support are written as

$$\sum_{k=0}^{\bar{N}} \overline{M}_{M'}(k) = 0 \tag{42.a}$$

$$\sum_{k=0}^{\bar{N}} \overline{T}_{M'}(k) = 0 \tag{42.b}$$

For pinned-pinned beam, substituting the boundary conditions expressed in Eqs. (37) and (40) into Eq. (35) and taking $Y_{1'}(1) = c_1, \Phi_{1'}(0) = c_2$; for cantilever beam, substituting the boundary conditions expressed in Eqs. (38) and (42) into Eq. (35) and taking $Y_{1'}(1) = c_1, \Phi_{1'}(1) = c_2$; for free-fixed beam, substituting the boundary conditions expressed in Eqs. (39) and (41) into Eq. (35) and taking $Y_{1'}(1) = c_1, Y_{1'}(1) = c_2$; the following matrix expression is obtained

$$\begin{bmatrix} A_{11}^{(\bar{N})}(\omega) & A_{12}^{(\bar{N})}(\omega) \\ A_{21}^{(\bar{N})}(\omega) & A_{22}^{(\bar{N})}(\omega) \end{bmatrix} \cdot \begin{Bmatrix} c_1 \\ c_2 \end{Bmatrix} = \begin{Bmatrix} 0 \\ 0 \end{Bmatrix} \tag{43}$$

where c_1 and c_2 are constants and $A_{a1}^{(\bar{N})}(\omega)$, $A_{a2}^{(\bar{N})}(\omega)$ (a=1, 2) are polynomials of ω corresponding $\overline{N}$.

In the last step, for non-trivial solution, equating the coefficient matrix that is given in Eq. (43) to zero one determines the natural frequencies of the vibrating system as is given in Eq. (44).

$$\begin{vmatrix} A_{11}^{(\bar{N})}(\omega) & A_{12}^{(\bar{N})}(\omega) \\ A_{21}^{(\bar{N})}(\omega) & A_{22}^{(\bar{N})}(\omega) \end{vmatrix} = 0 \tag{44}$$

The j^{th} estimated eigenvalue, $\omega_j^{(\bar{N})}$ corresponds to $\overline{N}$ and the value of $\overline{N}$ is determined as

$$\left| \omega_j^{(\bar{N})} - \omega_j^{(\bar{N}-1)} \right| \leq \varepsilon \tag{45}$$

where $\omega_j^{(\bar{N}-1)}$ is the j^{th} estimated eigenvalue corresponding to ($\overline{N} - 1$) and ε is the small tolerance parameter. If Eq. (45) is satisfied, the j^{th} estimated eigenvalue, $\bar{\omega}_j^{(N)}$ is obtained.

The procedure that is explained below can be used to plot the mode shapes of Timoshenko multiple-step beam. The following equalities can be written by using Eq. (43)

$$A_{11}(\omega)\cdot c_1 + A_{12}(\omega)\cdot c_2 = 0 \tag{46}$$

Using Eq. (46), the constant c_2 can be obtained in terms of c_1 as follows

$$c_2 = -\frac{A_{11}(\omega)}{A_{12}(\omega)}\cdot c_1 \tag{47}$$

All transformed functions can be expressed in terms of ω, c_1 and c_2. Since c_2 has been written in terms of c_1 above, $Y(k)$, $\Phi(k)$, $\overline{M}(k)$ and $\overline{T}(k)$ can be expressed in terms c_1 as follows

$$Y(k) = Y(\omega, c_1) \tag{48}$$

$$\Phi(k) = \Phi(\omega, c_1) \tag{49}$$

$$\overline{M}(k) = \overline{M}(\omega, c_1) \tag{50}$$

$$\overline{T}(k) = \overline{T}(\omega, c_1) \tag{51}$$

The mode shapes can be plotted for several values of ω by using Eq. (48).

5. Numerical analysis and discussions

In this study, three numerical examples are considered. For three numerical examples, the first five natural frequencies, $\omega_\alpha(\alpha=1(1)5)$ are calculated by using a computer program prepared by the author. In this program, the secant method is used in which determinant values are evaluated for a range (ω_α) values. The (ω_α) value causing a sign change between the successive determinant values is a root of frequency equation and means a frequency for the system.

Natural frequencies are found by determining values for which the determinant of the coefficient matrixes is equal to zero. There are various methods for calculating the roots of the frequency equation. One common used and simple technique is the secant method in which a linear interpolation is employed. The eigenvalues, the natural frequencies, are determined by a trial and error method based on interpolation and the bisection approach. One such procedure consists of evaluating the determinant for a range of frequency values, ω_α. When there is a change of sign between successive evaluations, there must be a root lying in this interval. The iterative computations are determined when the value of the determinant changed sign due to a change of 10^{-4} in the value of ω_α.

All numerical results of this paper are obtained based on a three-step Timoshenko beam with circular cross-sections. The dimensions of the three-step Timoshenko beam are presented in Fig. 2.

From Fig. 2 one sees that, the diameters of the segments are: d_1=0.10 m, d_2=0.15 m, d_3=0.20 m and d_4=0.25 m; the lengths of the segments are: $L_1=L_2=L_3=L_4$=0.50 m; the locations for the step changes in cross-sections are: $\bar{z}_1$=0.25, $\bar{z}_2$=0.50 and $\bar{z}_3$=0.75.

In all numerical examples, the mass density of the beam is taken as $\rho=7.8368\times10^3$ kg/m^3;

Young's modulus of the beam is taken as E=2.069×10^{11} N/m^2; the shear modulus of the beam is taken as G=7.95769×10^{10} N/m^2; the shape factor of the beam is taken as $\bar{k}$ =4/3 and the nondimensionalized multiplication factors for the axial compressive force are taken as N_r=0.0, 0.10 and 0.20.

5.1 Free vibration analysis of the axial-loaded and three-step Timoshenko beam carrying single intermediate lumped mass without rotary inertia

In the first numerical example the pinned-pinned, clamped-free and free-clamped Timoshenko beams carrying single intermediate lumped mass (m_1) without rotary inertia are considered. In this numerical example, the magnitude and locations of the intermediate lumped mass are taken as: m_1=(1.00$\cdot\bar{m}\cdot L$) located at z_1^*=0.375, z_2^*=0.625 and z_3^*=0.875, respectively.

Using DTM, the frequency values obtained for the first five modes of the pinned-pinned Timoshenko beam are presented in Table 4, for the first five modes of the clamped-free Timoshenko beam are presented in Table 5, and for the first five modes of the free-clamped Timoshenko beam are presented in Table 6 being compared with the frequency values obtained by using NAT for the different values of nondimensionalized multiplication factors for the axial compressive force (N_r).

For N_r=0.20, Figs. 3 and 4 show the first five mode shapes of the axial-loaded and three-step Timoshenko beam with pinned-pinned boundary condition. Fig. 3 is for the pinned-pinned and three-step Timoshenko beam without attachment, while Fig. 4 is for the pinned-pinned and three-

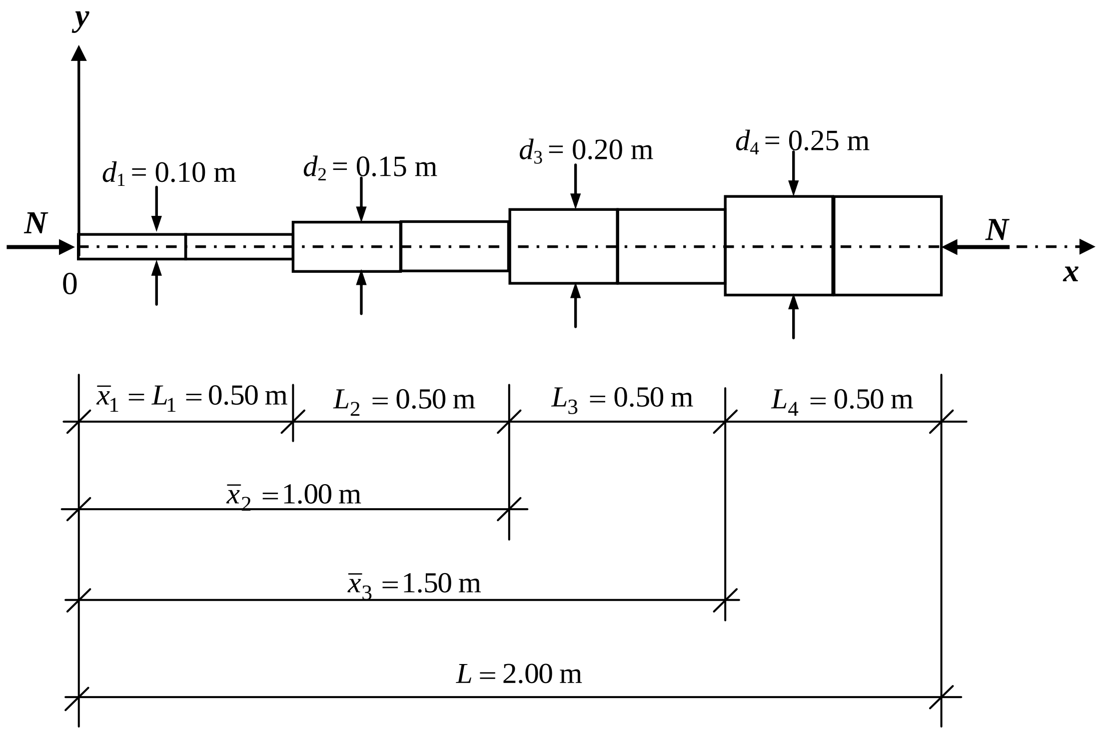

Fig. 2 The dimensions of the three-step Timoshenko beam

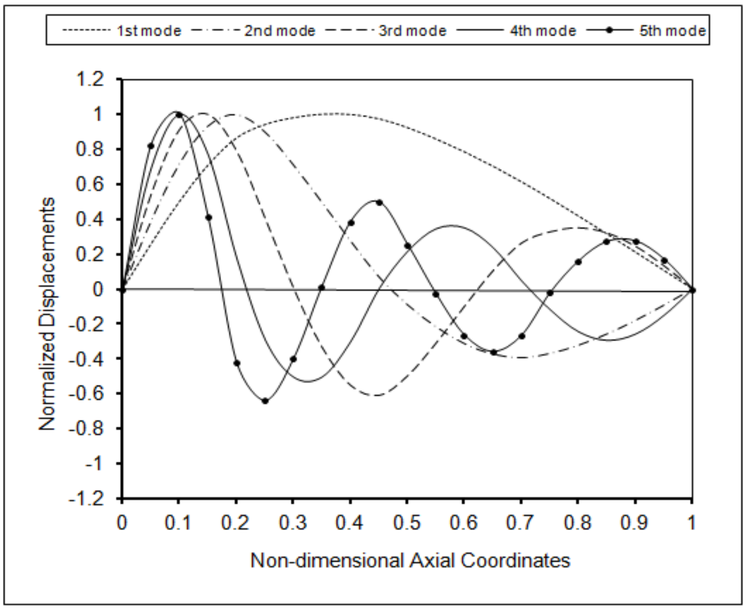

Fig. 3 The first five mode shapes of the pinned-pinned and three-step Timoshenko beam without attachment, N_r=0.20

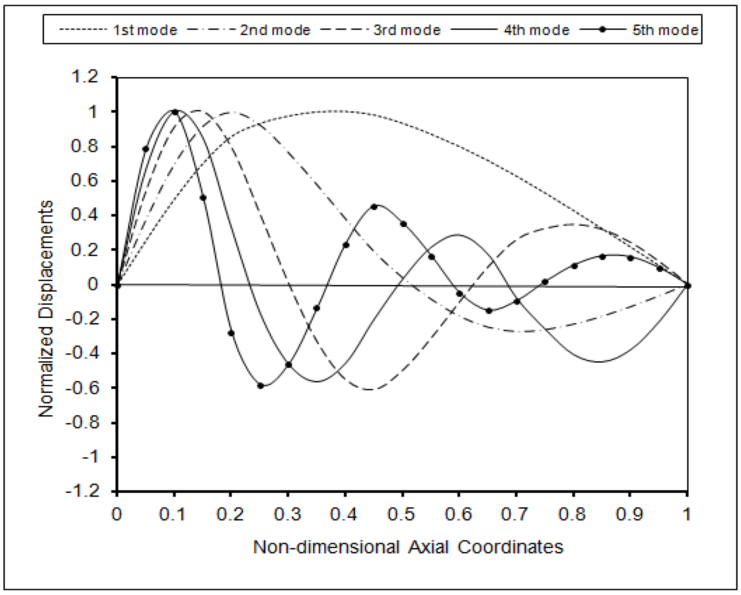

Fig. 4 The first five mode shapes of the pinned-pinned and three-step Timoshenko beam carrying one lumped mass located at z_1^*=0.625, N_r=0.20

step Timoshenko beam carrying one intermediate lumped mass located at z_1^*=0.625. For N_r=0.20, Figs. 5 and 6 show the first five mode shapes of the axial-loaded and three-step Timoshenko beam with clamped-free boundary condition. Fig. 5 is for the clamped-free and three-step Timoshenko beam without attachment, while Fig. 6 is for the clamped-free and three-step Timoshenko beam

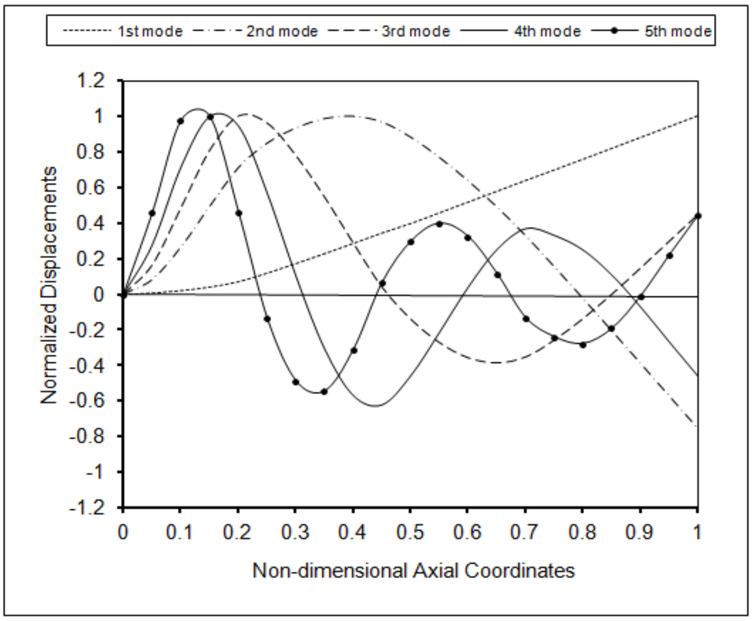

Fig. 5 The first five mode shapes of the cantilever and three-step Timoshenko beam without attachment, N_r=0.20

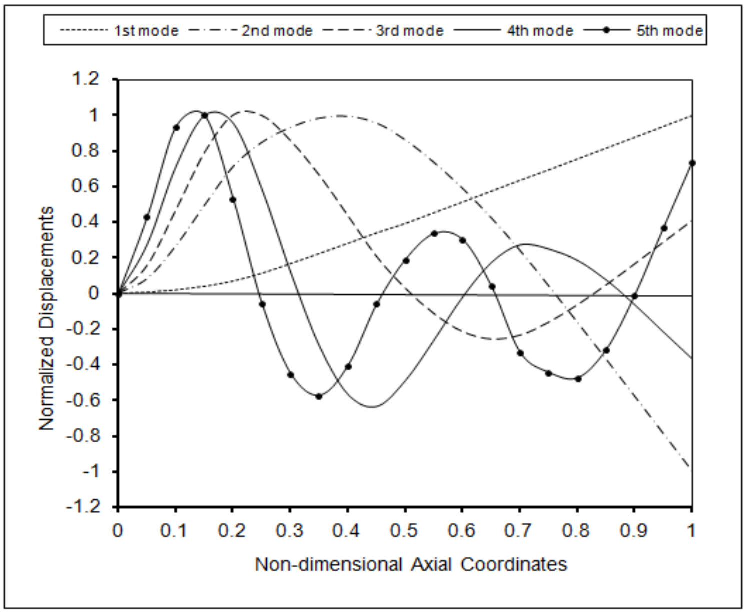

Fig. 6 The first five mode shapes of the cantilever and three-step Timoshenko beam carrying one lumped mass located at z_1^*=0.625, N_r=0.20

carrying one intermediate lumped mass located at z_1^*=0.625**.** For N_r=0.20, Figs. 7 and 8 show the first five mode shapes of the axial-loaded and three-step Timoshenko beam with free-clamped boundary condition. Fig. 7 is for the free-clamped and three-step Timoshenko beam without

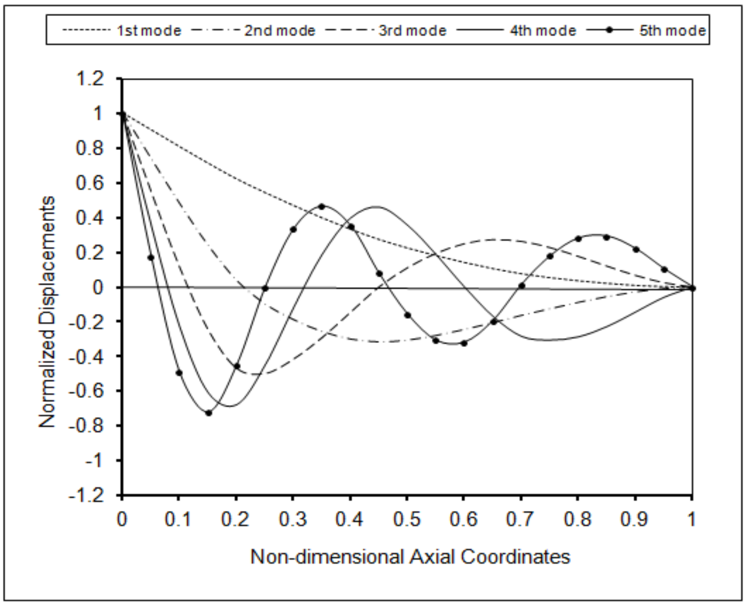

Fig. 7 The first five mode shapes of the free-clamped and three-step Timoshenko beam without attachment, N_r=0.20

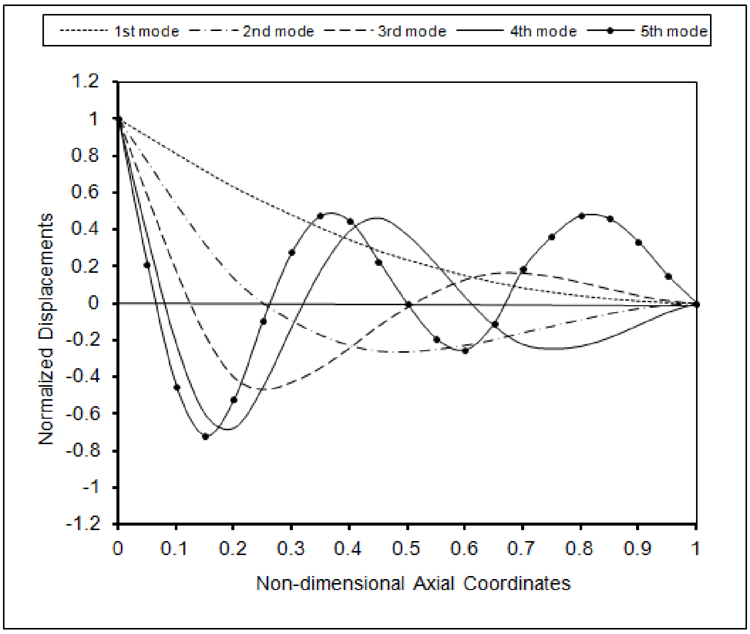

Fig. 8 The first five mode shapes of the free-clamped and three-step Timoshenko beam carrying one lumped mass located at z_1^*=0.625, N_r=0.20

attachment, while Fig. 8 is for the free-clamped and three-step Timoshenko beam carrying one intermediate lumped mass located at z_1^*=0.625**.**

From Tables 4-6, one can sees that increasing N_r causes an increase in the first five mode

Table 4 The first five natural frequencies of the pinned-pinned Timoshenko beam with three changes in cross-sections and carrying a lumped mass for different values of N_r

Location of lumped mass, $z_1^*=x_1^*/L$	ω_α (rad/sec)	METHOD	(BEBT) $N_r = 0.00$	(TBT) $N_r = 0.00$	(TBT) $N_r = 0.10$	(TBT) $N_r = 0.20$
*	ω_1	DTM ($\bar{N}$ =34)	423.9048	418.9494	420.0096	421.0676
		NAT	423.9048	418.9495	420.0088	421.0669
	ω_2	DTM ($\bar{N}$ =42)	2012.6557	1947.2010	1947.6836	1948.1640
		NAT	2012.6559	1947.2020	1947.6827	1948.1632
	ω_3	DTM ($\bar{N}$ =48)	4638.1343	4275.9113	4276.2926	4276.6746
		NAT	4638.1346	4275.9114	4276.2929	4276.6742
	ω_4	DTM ($\bar{N}$ =50)	8352.9477	7322.5740	7323.0841	7323.5952
		NAT	8352.9477	7322.5741	7323.0845	7323.5946
	ω_5	DTM ($\bar{N}$ =54)	12574.9954	10162.0529	10162.5983	10163.1434
		NAT	12574.9958	10162.0528	10162.5982	10163.1437
0.375	ω_1	DTM ($\bar{N}$ =34)	319.4341	316.5288	317.8596	319.1869
		NAT	319.4341	316.5288	317.8596	319.1866
	ω_2	DTM ($\bar{N}$ =42)	1853.3864	1789.4207	1790.0342	1790.6480
		NAT	1853.3864	1789.4207	1790.0343	1790.6477
	ω_3	DTM ($\bar{N}$ =48)	4110.1341	3825.8438	3826.1888	3826.5351
		NAT	4110.1341	3825.8438	3826.1892	3826.5344
	ω_4	DTM ($\bar{N}$ =50)	7709.5714	6642.9094	6643.4722	6644.0375
		NAT	7709.5714	6642.9093	6643.4732	6644.0368
	ω_5	DTM ($\bar{N}$ =54)	11621.7699	9886.6243	9887.2049	9887.7879
		NAT	11621.7699	9886.6243	9887.2055	9887.7868
0.625	ω_1	DTM ($\bar{N}$ =34)	356.0274	352.5251	353.6694	354.8120
		NAT	356.0275	352.5250	353.6699	354.8129
	ω_2	DTM ($\bar{N}$ =42)	1849.5144	1794.2629	1794.7777	1795.2931
		NAT	1849.5142	1794.2620	1794.7771	1795.2920
	ω_3	DTM ($\bar{N}$ =48)	4637.8405	4275.7922	4276.1747	4276.5567
		NAT	4637.8401	4275.7928	4276.1742	4276.5554
	ω_4	DTM ($\bar{N}$ =50)	7771.2653	6685.1369	6685.54774	6685.9594
		NAT	7771.2650	6685.1363	6685.5477	6685.9588
	ω_5	DTM ($\bar{N}$ =54)	11249.5949	9455.6282	9456.2819	9456.9341
		NAT	11249.5944	9455.6275	9456.2804	9456.9333
0.875	ω_1	DTM ($\bar{N}$ =34)	413.3018	408.6113	409.6698	410.7274
		NAT	413.3012	408.6111	409.6693	410.7262
	ω_2	DTM ($\bar{N}$ =42)	1917.3749	1856.3775	1856.8449	1857.3136
		NAT	1917.3742	1856.3772	1856.8450	1857.3127
	ω_3	DTM ($\bar{N}$ =48)	4285.5914	3950.0631	3950.4235	3950.7829
		NAT	4285.5916	3950.0636	3950.4224	3950.7810
	ω_4	DTM ($\bar{N}$ =50)	7812.7115	6687.0796	6687.4973	6687.9150
		NAT	7812.7113	6687.0789	6687.4971	6687.9151
	ω_5	DTM ($\bar{N}$ =54)	11490.8391	9473.5058	9474.1266	9474.7476
		NAT	11490.8385	9473.5052	9474.1259	9474.7466

*For the case of m_1=0

frequency values for three different boundary conditions, as expected. The frequency values obtained for the Timoshenko beam without the axial force effect are less than the values obtained for the Bernoulli-Euler beam as expected, since the shear deformation is considered in TBT. As the intermediate lumped mass is acted to the beam for N_r is being constant, the first five frequency values are decreased for all boundary conditions. This is a reasonable result, because in this situation, the displacements and so that the periods of the beam are increased.

In application of DTM, the natural frequency values of the beams are calculated by increasing series size $\overline{N}$. In Tables 4-6, convergences of the first five natural frequencies are introduced. Here, it is seen that; for pinned-pinned beam, when the series size is taken 54; for clamped-free

Table 5 The first five natural frequencies of the cantilever Timoshenko beam with three changes in cross-sections and carrying a lumped mass for different values of N_r.

Location of lumped mass, $z_1^*=x_1^*/L$	ω_α (rad/sec)	METHOD	(BEBT) N_r=0.00	(TBT) N_r=0.00	(TBT) N_r=0.10	(TBT) N_r=0.20
*	ω_1	**DTM** ($\overline{N}$=38)	56.4543	56.3053	57.3894	58.4481
		NAT	56.4543	56.3052	57.3888	58.4486
	ω_2	**DTM** ($\overline{N}$=46)	834.1811	805.3909	806.8320	808.2732
		NAT	834.1810	805.3901	806.8326	808.2726
	ω_3	**DTM** ($\overline{N}$=52)	2960.8740	2798.9821	2799.7319	2800.4798
		NAT	2960.8742	2798.9829	2799.7311	2800.4793
	ω_4	**DTM** ($\overline{N}$=58)	6073.5394	5498.5509	5499.0138	5499.4762
		NAT	6073.5389	5498.5515	5499.0141	5499.4766
	ω_5	**DTM** ($\overline{N}$=62)	10600.8083	9051.2237	9051.7383	9052.2524
		NAT	10600.8083	9051.2237	9051.7384	9052.2528
0.375	ω_1	**DTM** ($\overline{N}$=38)	55.1250	54.9798	56.1426	57.2742
		NAT	55.1252	54.9800	56.1428	57.2746
	ω_2	**DTM** ($\overline{N}$=46)	616.6014	598.7798	600.6597	602.5338
		NAT	616.6019	598.7795	600.6598	602.5344
	ω_3	**DTM** ($\overline{N}$=52)	2702.3241	2552.4541	2553.2646	2554.0740
		NAT	2702.3239	2552.4545	2553.2644	2554.0744
	ω_4	**DTM** ($\overline{N}$=58)	5483.2364	4954.7431	4955.2019	4955.6598
		NAT	5483.2371	4954.7440	4955.2016	4955.6591
	ω_5	**DTM** ($\overline{N}$=62)	9570.9587	8221.0488	8221.6434	8222.2378
		NAT	9570.9588	8221.0485	8221.6425	8222.2363
0.625	ω_1	**DTM** ($\overline{N}$=38)	51.3966	51.2740	52.4705	53.6348
		NAT	51.3966	51.2740	52.4704	53.6342
	ω_2	**DTM** ($\overline{N}$=46)	752.3899	728.6084	730.0509	731.4928
		NAT	752.3895	728.6090	730.0518	731.4920
	ω_3	**DTM** ($\overline{N}$=52)	2687.6819	2549.4691	2550.2700	2551.0711
		NAT	2687.6819	2549.4690	2550.2704	2551.0717
	ω_4	**DTM** ($\overline{N}$=58)	6003.4198	5415.5676	5416.0290	5416.4900
		NAT	6003.4197	5415.5675	5416.0290	5416.4905
	ω_5	**DTM** ($\overline{N}$=62)	10139.8644	8630.5038	8630.9229	8631.3424
		NAT	10139.8645	8630.5031	8630.9223	8631.3413

Table 5 Continued

0.875	ω_1	**DTM** ($\bar{N}$ =38)	46.3953	46.3030	47.4404	48.5466
		NAT	46.3953	46.3030	47.4404	48.5466
	ω_2	**DTM** ($\bar{N}$ =46)	812.7784	785.7517	787.2210	788.6878
		NAT	812.7784	785.7517	787.2210	788.6878
	ω_3	**DTM** ($\bar{N}$ =52)	2952.2398	2789.0856	2789.8405	2790.5957
		NAT	2952.2394	2789.0849	2789.8399	2790.5948
	ω_4	**DTM** ($\bar{N}$ =58)	6061.9262	5496.9991	5497.4618	5497.9218
		NAT	6061.9262	5496.9991	5497.4606	5497.9220
	ω_5	**DTM** ($\bar{N}$ =62)	10454.8614	8941.0095	8941.4770	8941.9442
		NAT	10454.8613	8941.0099	8941.4776	8941.9450

*For the case of m_1=0

Table 6 The first five natural frequencies of the free-clamped Timoshenko beam with three changes in cross-sections and carrying a lumped mass for different values of N_r

Location of lumped mass, $z_1^*=x_1^*/L$	ω_α (rad/sec)	METHOD	(BEBT) N_r=0.00	(TBT) N_r=0.00	(TBT) N_r=0.10	(TBT) N_r=0.20
*	ω_1	**DTM** ($\bar{N}$ =36)	461.5130	457.1752	458.1299	459.0814
		NAT	461.5130	457.1750	458.1296	459.0803
	ω_2	**DTM** ($\bar{N}$ =44)	1442.3630	1395.8694	1396.9639	1398.0580
		NAT	1442.3630	1395.8691	1396.9636	1398.0572
	ω_3	**DTM** ($\bar{N}$ =52)	3234.0073	3008.5049	3009.2761	3010.0468
		NAT	3234.0074	3008.5045	3009.2752	3010.0459
	ω_4	**DTM** ($\bar{N}$ =56)	6188.2742	5370.9840	5371.4239	5371.8631
		NAT	6188.2740	5370.9844	5371.4233	5371.8622
	ω_5	**DTM** ($\bar{N}$ =60)	10581.3341	8645.3090	8645.7068	8646.1048
		NAT	10581.3339	8645.3088	8645.7064	8646.1037
0.375	ω_1	**DTM** ($\bar{N}$ =36)	371.5354	367.9440	368.8474	369.7475
		NAT	371.5354	367.9440	368.8474	369.7473
	ω_2	**DTM** ($\bar{N}$ =44)	1243.9063	1216.6220	1218.0334	1219.4425
		NAT	1243.9063	1216.6220	1218.0334	1219.4426
	ω_3	**DTM** ($\bar{N}$ =52)	3082.0846	2827.0352	2827.7824	2828.5311
		NAT	3082.0846	2827.0352	2827.7827	2828.5302
	ω_4	**DTM** ($\bar{N}$ =56)	5541.1410	4957.9240	4958.3938	4958.8612
		NAT	5541.1410	4957.9241	4958.3932	4958.8623
	ω_5	**DTM** ($\bar{N}$ =60)	9599.3810	7673.7578	7674.2559	7674.7520
		NAT	9599.3811	7673.7573	7674.2553	7674.7531
0.625	ω_1	**DTM** ($\bar{N}$ =36)	448.3169	443.7184	444.6269	445.5315
		NAT	448.3169	443.7184	444.6269	445.5316
	ω_2	**DTM** ($\bar{N}$ =44)	1261.6793	1219.4420	1220.4996	1221.5562
		NAT	1261.6793	1219.4420	1220.4996	1221.5559
	ω_3	**DTM** ($\bar{N}$ =52)	2840.5989	2681.0260	2681.9454	2682.8668
		NAT	2840.5990	2681.0260	2681.9456	2682.8652
	ω_4	**DTM** ($\bar{N}$ =56)	6054.5019	5325.8814	5326.3419	5326.8017
		NAT	6054.5020	5325.8816	5326.3410	5326.8004
	ω_5	**DTM** ($\bar{N}$ =60)	10191.8727	7978.1175	7978.4368	7978.7553
		NAT	10191.8725	7978.1182	7978.4363	7978.7542

Table 6 Contined

0.875	ω_1	**DTM** ($\bar{N}$ =36)	461.3359	456.9713	457.9243	458.8738
		NAT	461.3359	456.9710	457.9241	458.8733
	ω_2	**DTM** ($\bar{N}$ =44)	1436.8977	1388.8416	1389.9234	1391.0022
		NAT	1436.8977	1388.8417	1389.9228	1391.0029
	ω_3	**DTM** ($\bar{N}$ =52)	3181.0297	2937.3678	2938.1071	2938.8492
		NAT	3181.0296	2937.3674	2938.1077	2938.8481
	ω_4	**DTM** ($\bar{N}$ =56)	5882.1422	5016.9318	5017.3460	5017.7581
		NAT	5882.1424	5016.9312	5017.3453	5017.7595
	ω_5	**DTM** ($\bar{N}$ =60)	9937.3220	7687.6788	7687.9852	7688.2938
		NAT	9937.3226	7687.6798	7687.9860	7688.2922

*For the case of m_1=0

beam, when the series size is taken 62 and for free-clamped beam, when the series size is taken 60, the natural frequency values of the fifth mode can be appeared. Additionally, here it is seen that higher modes appear when more terms are taken into account in DTM applications. Thus, depending on the order of the required mode, one must try a few values for the term number at the beginning of the calculations in order to find the adequate number of terms.

5.2 Free vibration analysis of the axial-loaded and three-step Timoshenko beam carrying single rotary inertia without intermediate lumped mass

In the second numerical example the pinned-pinned, clamped-free and free-clamped Timoshenko beams carrying single rotary inertia ($I_{0,1}$) without intermediate lumped mass are considered. In this numerical example, the magnitude and locations of the rotary inertia are taken as: $I_{0,1}$=($0.01\cdot \bar{m}_1 \cdot L^3$) located at $\hat{z}_1$=0.375, $\hat{z}_2$=0.625 and $\hat{z}_3$=0.875, respectively.

Using DTM, the frequency values obtained for the first five modes of the axial-loaded and three-step Timoshenko beam with pinned-pinned, clamped-free and free-clamped boundary conditions are presented in Tables 7, 8 and 9, respectively, being compared with the frequency values obtained by using NAT for the different values of nondimensionalized multiplication factors for the axial compressive force (N_r).

From Tables 7-9, it can be seen that, as the axial compressive force acting to the beam is increased, the first five mode frequency values for three boundary conditions are increased.

In application of DTM, the natural frequency values of the beams are calculated by increasing series size $\bar{N}$. In Tables 7-9, convergences of the first five natural frequencies are introduced. Here, it is seen that; for pinned-pinned beam, when the series size is taken 54; for clamped-free beam, when the series size is taken 60 and for free-clamped beam, when the series size is taken 58, the natural frequency values of the fifth mode can be appeared.

5.3 Free vibration analysis of the axial-loaded and three-step Timoshenko beam carrying three intermediate lumped masses and/or three rotary inertias

In the third numerical example; the pinned-pinned, clamped-free and free-clamped Timoshenko beams carrying three intermediate lumped masses (m_1, m_2, m_3) and/or three rotary inertias ($I_{0,1}$, $I_{0,2}$,

$I_{0,3}$) are considered. In this numerical example, two different cases are studied. For the first case; the beam carries only three intermediate lumped masses. In this case, the magnitudes and locations of the intermediate lumped masses are taken as: $m_1=m_2=m_3=(1.00\cdot\overline{m}_1\cdot L)$ located at $z_1^*=0.375$, $z_2^*=0.625$ and $z_3^*=0.875$, respectively. For the second case; the beam carries three intermediate lumped masses and three rotary inertias. In this case, the magnitudes and locations of the intermediate lumped masses and rotary inertias are taken as: $m_1=m_2=m_3=(1.00\cdot\overline{m}_1\cdot L)$, $I_{0,1}=I_{0,2}=I_{0,3}=(0.01\cdot\overline{m}_1\cdot L^3)$ located at $z_1^*=\hat{z}_1=0.375$, $z_3^*=\hat{z}_3=0.625$ and $z_1^*=\hat{z}_1=0.875$, respectively.

Table 7 The first five natural frequencies of the pinned-pinned Timoshenko beam with three changes in cross-sections and with single rotary inertia for different values of N_r

Location of lumped mass, $z_1^*=x_1^*/L$	ω_α (rad/sec)	METHOD	(BEBT) N_r=0.00	(TBT)		
				N_r=0.00	N_r=0.10	N_r=0.20
0.375	ω_1	DTM ($\overline{N}$=34)	423.9012	418.9430	420.0045	421.0618
		NAT	423.9010	418.9435	420.0038	421.0627
	ω_2	DTM ($\overline{N}$=42)	1632.7664	1611.7041	1612.1111	1612.5196
		NAT	1632.7664	1611.7041	1612.1111	1612.5182
	ω_3	DTM ($\overline{N}$=48)	3766.7278	3541.1114	3541.5556	3541.9984
		NAT	3766.7277	3541.1112	3541.5553	3541.9995
	ω_4	DTM ($\overline{N}$=52)	6036.8610	5598.9681	5599.4379	5599.9047
		NAT	6036.8602	5598.9683	5599.4373	5599.9058
	ω_5	DTM ($\overline{N}$=54)	9807.0239	7827.8997	7828.2820	7828.6644
		NAT	9807.0239	7827.8997	7828.2819	7828.6639
0.625	ω_1	DTM ($\overline{N}$=34)	419.694	414.8865	415.9529	417.0183
		NAT	419.6955	414.8865	415.9528	417.0178
	ω_2	DTM ($\overline{N}$=42)	1980.1535	1918.8699	1919.3264	1919.7836
		NAT	1980.1536	1918.8690	1919.3260	1919.7828
	ω_3	DTM ($\overline{N}$=48)	3808.6405	3690.8707	3691.2134	3691.5596
		NAT	3808.6399	3690.8698	3691.2140	3691.5581
	ω_4	DTM ($\overline{N}$=52)	7479.9365	6843.5165	6844.0450	6844.5731
		NAT	7479.9365	6843.5165	6844.0450	6844.5731
	ω_5	DTM ($\overline{N}$=54)	10978.0630	8740.3387	8740.5457	8740.7534
		NAT	10978.0629	8740.3385	8740.5458	8740.7532
0.875	ω_1	DTM ($\overline{N}$=34)	417.1940	412.4990	413.5581	414.6178
		NAT	417.1941	412.4993	413.5589	414.6174
	ω_2	DTM ($\overline{N}$=42)	1962.5020	1905.9285	1906.4102	1906.8919
		NAT	1962.5020	1905.9286	1906.4102	1906.8917
	ω_3	DTM ($\overline{N}$=48)	4509.0212	4200.1526	4200.5434	4200.9367
		NAT	4509.0209	4200.1522	4200.5440	4200.9355
	ω_4	DTM ($\overline{N}$=52)	8271.3273	7293.9294	7294.4527	7294.9738
		NAT	8271.3270	7293.9300	7294.4511	7294.9720
	ω_5	DTM ($\overline{N}$=54)	12565.3279	10152.6587	10153.1849	10153.7222
		NAT	12565.3279	10152.6587	10153.1857	10153.7218

Table 8 The first five natural frequencies of the cantilever Timoshenko beam with three changes in cross-sections and with single rotary inertia for different values of N_r

Location of lumped mass, $z_1^*=x_1^*/L$	ω_α (rad/sec)	METHOD	(BEBT) N_r=0.00	(TBT) N_r=0.00	(TBT) N_r=0.10	(TBT) N_r=0.20
0.375	ω_1	DTM ($\bar{N}$=38)	56.2276	56.0804	57.1560	58.2078
		NAT	56.2276	56.0807	57.1564	58.2084
	ω_2	DTM ($\bar{N}$=46)	833.8913	805.2655	806.6982	808.1280
		NAT	833.8913	805.2655	806.6983	808.1283
	ω_3	DTM ($\bar{N}$=52)	2185.4953	2138.1515	2138.8562	2139.5650
		NAT	2185.4953	2138.1515	2138.8574	2139.5636
	ω_4	DTM ($\bar{N}$=56)	4679.3441	4340.8275	4341.3359	4341.8447
		NAT	4679.3440	4340.8276	4341.3355	4341.8434
	ω_5	DTM ($\bar{N}$=60)	7840.6684	6853.5644	6854.0036	6854.4459
		NAT	7840.6682	6853.5641	6854.0045	6854.4445
0.625	ω_1	DTM ($\bar{N}$=38)	56.2001	56.0536	57.1286	58.1804
		NAT	56.2002	56.0536	57.1282	58.1791
	ω_2	DTM ($\bar{N}$=46)	804.3480	778.1856	779.6499	781.1116
		NAT	804.3483	778.1857	779.6495	781.1108
	ω_3	DTM ($\bar{N}$=52)	2948.7688	2790.8717	2791.5973	2792.3259
		NAT	2948.7688	2790.8717	2791.5982	2792.3246
	ω_4	DTM ($\bar{N}$=56)	4748.4793	4632.5326	4632.9509	4633.3680
		NAT	4748.4794	4632.5325	4632.9504	4633.3683
	ω_5	DTM ($\bar{N}$=60)	8847.1946	7701.0811	7701.4875	7701.8935
		NAT	8847.1942	7701.0807	7701.4868	7701.8926
0.875	ω_1	DTM ($\bar{N}$=38)	56.1969	56.0503	57.1247	58.1754
		NAT	56.1969	56.0503	57.1247	58.1754
	ω_2	DTM ($\bar{N}$=46)	788.5650	764.1013	765.5276	766.9513
		NAT	788.5650	764.1013	765.5276	766.9513
	ω_3	DTM ($\bar{N}$=52)	2707.2935	2595.0536	2595.7860	2596.5198
		NAT	2707.2935	2595.0536	2595.7865	2596.5193
	ω_4	DTM ($\bar{N}$=56)	5377.9510	5008.0436	5008.5179	5008.9957
		NAT	5377.9504	5008.0430	5008.5187	5008.9944
	ω_5	DTM ($\bar{N}$=60)	9787.3082	8277.1557	8277.5683	8277.9774
		NAT	9787.3079	8277.1561	8277.5675	8277.9786

Table 9 The first five natural frequencies of the free-clamped Timoshenko beam with three changes in cross-sections and with single rotary inertia for different values of N_r

Location of lumped mass, $z_1^*=x_1^*/L$	ω_α (rad/sec)	METHOD	(BEBT) N_r=0.00	(TBT) N_r=0.00	(TBT) N_r=0.10	(TBT) N_r=0.20
0.375	ω_1	DTM ($\bar{N}$=36)	446.0660	442.4513	443.3527	444.2513
		NAT	446.0659	442.4513	443.3529	444.2506
	ω_2	DTM ($\bar{N}$=46)	1409.1399	1361.3431	1362.2625	1363.1804
		NAT	1409.1399	1361.3431	1362.2622	1363.1800
	ω_3	DTM ($\bar{N}$=50)	2451.6606	2413.5054	2414.4628	2415.4210
		NAT	2451.6605	2413.5058	2414.4637	2415.4221

Table 9 Continued

0.375	ω_4	DTM ($\bar{N}$ =54)	4931.1577	4288.4994	4288.9101	4289.3213
		NAT	4931.1576	4288.4991	4288.9097	4289.3204
	ω_5	DTM ($\bar{N}$ =58)	7752.4304	6899.9765	6900.4102	6900.8439
		NAT	7752.4304	6899.9765	6900.4101	6900.8435
0.625	ω_1	DTM ($\bar{N}$ =36)	457.1416	452.9944	453.9262	454.8568
		NAT	457.1416	452.9946	453.9271	454.8556
	ω_2	DTM ($\bar{N}$ =46)	1411.7109	1372.1336	1373.2375	1374.3397
		NAT	1411.7100	1372.1333	1373.2366	1374.3389
	ω_3	DTM ($\bar{N}$ =50)	3227.0156	2987.9685	2988.6867	2989.4050
		NAT	3227.0157	2987.9685	2988.6859	2989.4034
	ω_4	DTM ($\bar{N}$ =54)	4781.4130	4488.7990	4489.2316	4489.6638
		NAT	4781.4122	4488.7982	4489.2306	4489.6631
	ω_5	DTM ($\bar{N}$ =58)	8799.6974	7774.3161	7774.7115	7775.1068
		NAT	8799.6975	7774.3161	7774.7109	7775.1055
0.875	ω_1	DTM ($\bar{N}$ =36)	461.0895	456.7648	457.7167	458.6649
		NAT	461.0895	456.7641	457.7159	458.6637
	ω_2	DTM ($\bar{N}$ =46)	1430.4980	1385.7016	1386.7819	1387.8590
		NAT	1430.4974	1385.7016	1386.7801	1387.8575
	ω_3	DTM ($\bar{N}$ =50)	3136.0608	2946.9945	2947.7568	2948.5174
		NAT	3136.0603	2946.9943	2947.7557	2948.5171
	ω_4	DTM ($\bar{N}$ =54)	5762.9677	5232.7760	5233.2354	5233.6928
		NAT	5762.9677	5232.7766	5233.2347	5233.6927
	ω_5	DTM ($\bar{N}$ =58)	9962.1583	8537.7533	8538.1578	8538.5626
		NAT	9962.1584	8537.7533	8538.1576	8538.5616

Using DTM, the frequency values obtained for the first five modes of the pinned-pinned Timoshenko beam are presented in Table 10, for the first five modes of the clamped-free Timoshenko beam are presented in Table 11, and for the first five modes of the free-clamped Timoshenko beam are presented in Table 12 being compared with the frequency values obtained by using NAT for the different values of nondimensionalized multiplication factors for the axial compressive force (N_r).

For N_r=0.20, Figs. 9 and 10 show the first five mode shapes of the axial-loaded and three-step Timoshenko beam with pinned-pinned boundary condition. Fig. 9 is for the pinned-pinned and three-step Timoshenko beam carrying three intermediate lumped masses without rotary inertias, while Fig. 10 is for the pinned-pinned and three-step Timoshenko beam carrying three intermediate lumped masses and three rotary inertias. For N_r=0.20, Figs. 11 and 12 show the first five mode shapes of the axial-loaded and three-step Timoshenko beam with clamped-free boundary condition. Fig. 11 is for the clamped-free and three-step Timoshenko beam carrying three intermediate lumped masses without rotary inertias, while Fig. 12 is for the clamped-free and three-step Timoshenko beam carrying three intermediate lumped masses and three rotary inertias. For N_r=0.20, Figs. 13 and 14 show the first five mode shapes of the axial-loaded and three-step Timoshenko beam with free-clamped boundary condition. Fig. 13 is for the free-clamped and three-step Timoshenko beam carrying three intermediate lumped masses without rotary inertias, while Fig. 14 is for the free-clamped and three-step Timoshenko beam carrying three intermediate

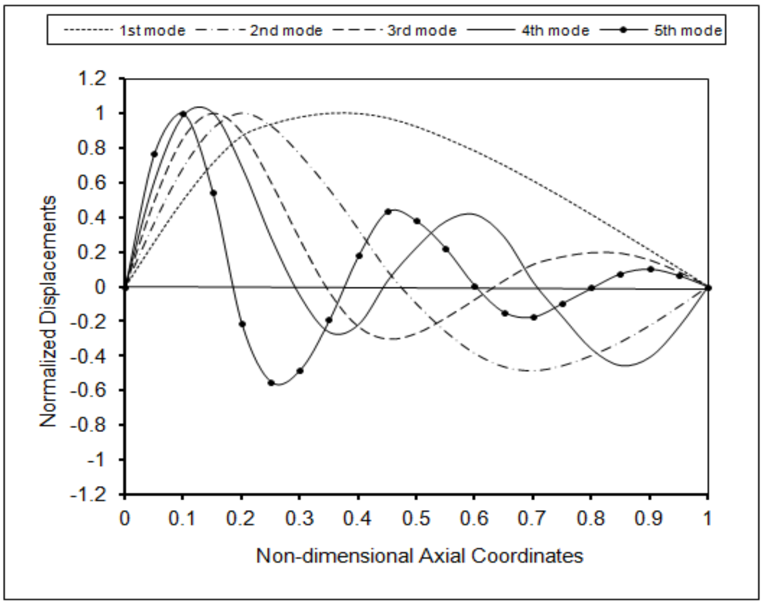

Fig. 9 The first five mode shapes of the pinned-pinned and three-step Timoshenko beam carrying three lumped masses, N_r=0.20

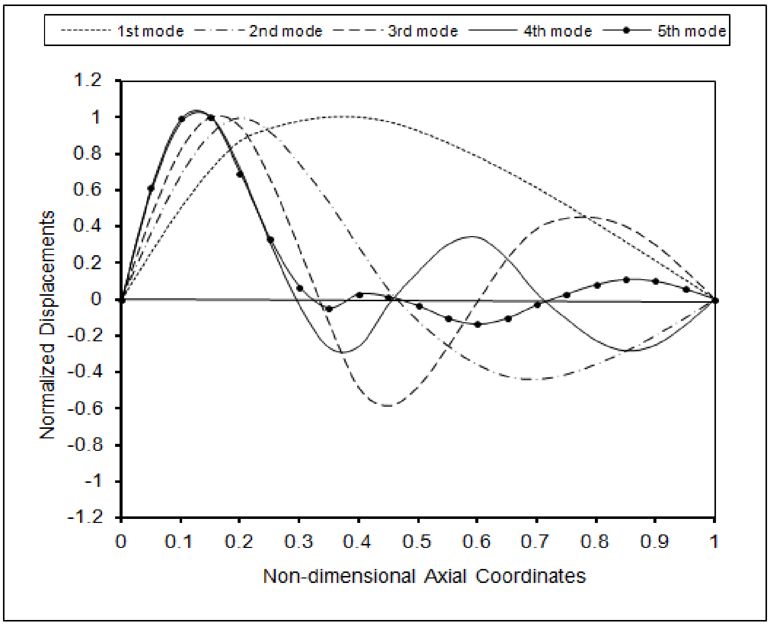

Fig. 10 The first five mode shapes of the pinned-pinned and three-step Timoshenko beam carrying three lumped masses together with three rotary inertias, N_r = 0.20

lumped masses and three rotary inertias.

It can be seen from Tables 10-12 that, as the axial compressive force acting to the beam is increased, the first five natural frequency values of the axial-loaded and three-step Timoshenko

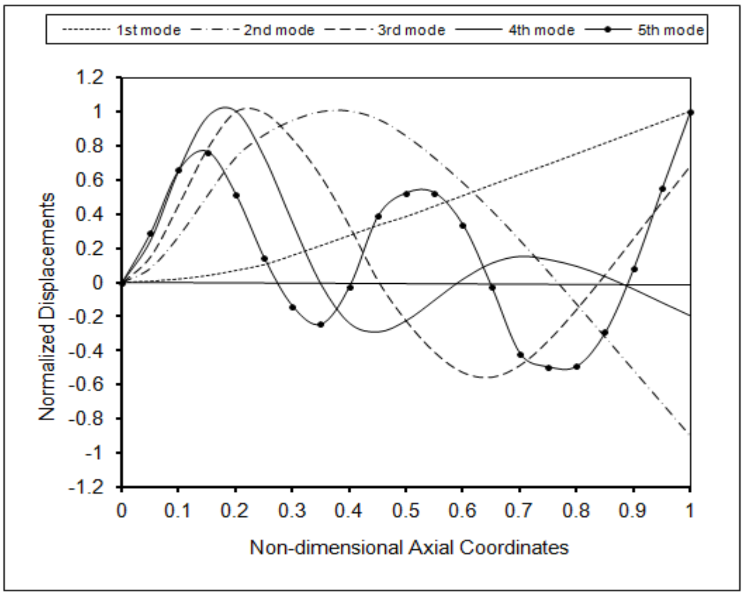

Fig. 11 The first five mode shapes of the cantilever and three-step Timoshenko beam carrying three lumped masses, N_r=0.20

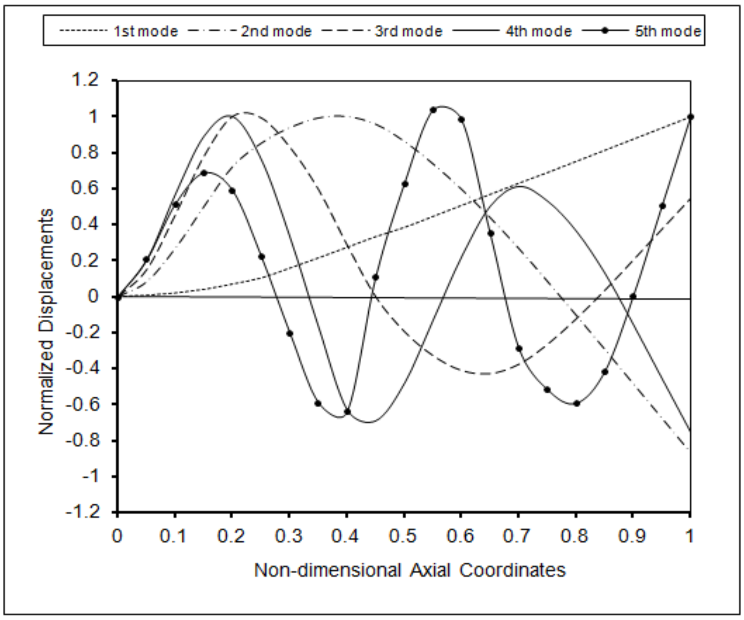

Fig. 12 The first five mode shapes of the cantilever and three-step Timoshenko beam carrying three lumped masses together with three rotary inertias, N_r = 0.20

beam with pinned-pinned, clamped-free and free-clamped boundary conditions are increased. As the rotary inertias are acted to the beam for N_r is being constant, all natural frequency values of Timoshenko beams are decreased for three different boundary conditions. This is a reasonable

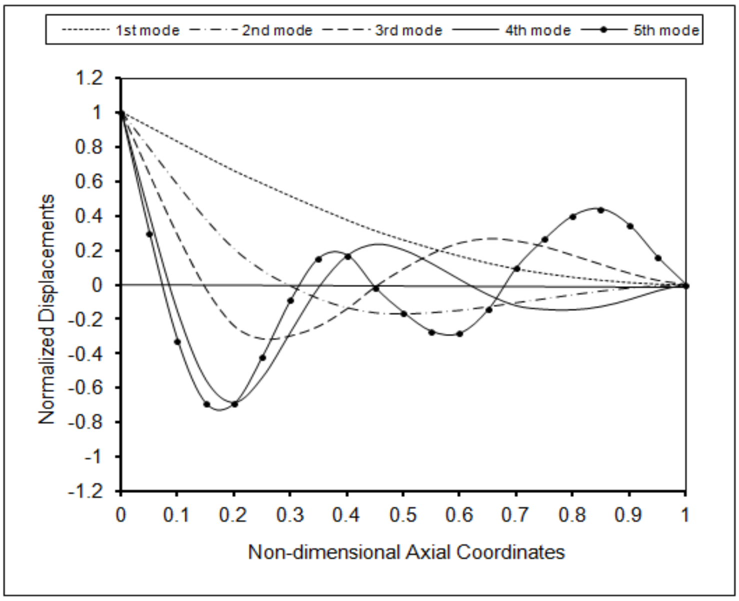

Fig. 13 The first five mode shapes of the free-clamped and three-step Timoshenko beam carrying three lumped masses, N_r=0.20

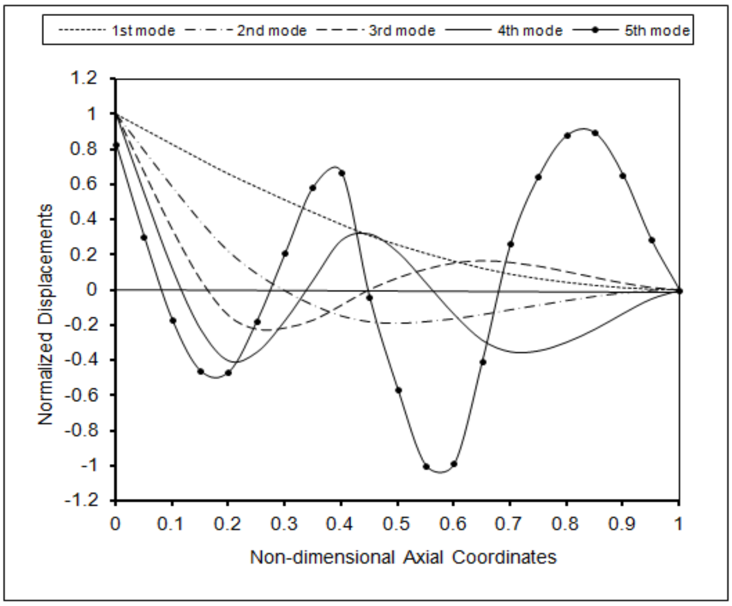

Fig. 14 The first five mode shapes of the free-clamped and three-step Timoshenko beam carrying three lumped masses together with three rotary inertias, N_r=0.20

result, because in this situation, the displacements and so that the periods of the beam are increased.

In application of DTM, the natural frequency values of the beams are calculated by increasing series size $\overline{N}$. In Tables 10-12, convergences of the first five natural frequencies are introduced. Here, it is seen that; for pinned-pinned beam, when the series size is taken 60; for clamped-free beam, when the series size is taken 70 and for free-clamped beam, when the series size is taken 68, the natural frequency values of the fifth mode can be appeared. Additionally, here it is seen that higher modes appear when more terms are taken into account in DTM applications.

Table 10 The first five natural frequencies of the pinned-pinned Timoshenko beam with three changes in cross-sections and carrying three lumped mass and/or three rotary inertias for different values of N_r

Attachments m_n, $I_{0,s}$ (n=s=1, 2, 3)	ω_α (rad/sec)	METHOD	(BEBT) N_r=0.00	(TBT) N_r=0.00	(TBT) N_r=0.10	(TBT) N_r=0.20
m_n	ω_1	DTM ($\overline{N}$=38)	284.5443	282.1787	283.5490	284.9168
		NAT	284.5444	282.1789	283.5499	284.9162
	ω_2	DTM ($\overline{N}$=46)	1540.4575	1494.1636	1494.8571	1495.5529
		NAT	1540.4573	1494.1635	1494.8579	1495.5520
	ω_3	DTM ($\overline{N}$=50)	3918.5378	3653.2225	3653.5449	3653.8672
		NAT	3918.5373	3653.2219	3653.5443	3653.8664
	ω_4	DTM ($\overline{N}$=56)	6098.9910	5217.9438	5218.3762	5218.8061
		NAT	6098.9919	5217.9431	5218.3753	5218.8072
	ω_5	DTM ($\overline{N}$=60)	10574.6797	9163.0789	9163.7748	9164.4671
		NAT	10574.6788	9163.0782	9163.7733	9164.4684
m_n, $I_{0,s}$	ω_1	DTM ($\overline{N}$=38)	281.2446	278.9596	280.3356	281.7069
		NAT	281.2446	278.9596	280.3351	281.7057
	ω_2	DTM ($\overline{N}$=46)	1352.4144	1329.7706	1330.3570	1330.9435
		NAT	1352.4144	1329.7707	1330.3567	1330.9427
	ω_3	DTM ($\overline{N}$=50)	2775.1731	2710.5750	2710.9296	2711.2840
		NAT	2775.1730	2710.5757	2710.9289	2711.2822
	ω_4	DTM ($\overline{N}$=56)	5591.9247	5041.3045	5041.8237	5042.3400
		NAT	5591.9250	5041.3044	5041.8229	5042.3411
	ω_5	DTM ($\overline{N}$=60)	6008.5274	5390.4820	5390.9623	5391.4421
		NAT	6008.5288	5390.4821	5390.9625	5391.4425

Table 11 The first five natural frequencies of the cantilever Timoshenko beam with three changes in cross-sections and carrying three lumped mass and/or three rotary inertias for different values of N_r

Attachments m_n, $I_{0,s}$ (n=s=1, 2, 3)	ω_α (rad/sec)	METHOD	(BEBT) N_r=0.00	(TBT) N_r=0.00	(TBT) N_r=0.10	(TBT) N_r=0.20
m_n	ω_1	DTM ($\overline{N}$=42)	42.8529	42.7712	44.0625	45.3068
		NAT	42.8529	42.7712	44.0623	45.3060
	ω_2	DTM ($\overline{N}$=50)	565.9431	550.9221	552.8258	554.7207
		NAT	565.9431	550.9222	552.8252	554.7216
	ω_3	DTM ($\overline{N}$=54)	2253.8761	2140.9554	2141.8722	2142.7894
		NAT	2253.8760	2140.9552	2141.8725	2142.7889
	ω_4	DTM ($\overline{N}$=62)	5393.5935	4869.4082	4869.8660	4870.3239
		NAT	5393.5936	4869.4086	4869.8652	4870.3233

Table 11 Continued

m_n	ω_5	DTM ($\bar{N}$ =70)	9032.8189	7901.7277	7902.2209	7902.7147
		NAT	9032.8188	7901.7281	7902.2219	7902.7136
m_n , $I_{0,s}$	ω_1	DTM ($\bar{N}$ =42)	42.5326	42.4532	43.7250	44.9495
		NAT	42.5325	42.4532	43.7245	44.9486
	ω_2	DTM ($\bar{N}$ =50)	541.0259	527.6540	529.5587	531.4584
		NAT	541.0257	527.6543	529.5596	531.4576
	ω_3	DTM ($\bar{N}$ =54)	1842.1150	1794.8317	1795.6731	1796.5188
		NAT	1842.1149	1794.8308	1795.6741	1796.5176
	ω_4	DTM ($\bar{N}$ =62)	3258.3858	3183.9040	3184.3599	3184.8190
		NAT	3258.3856	3183.9040	3184.3606	3184.8173
	ω_5	DTM ($\bar{N}$ =70)	6264.6768	5771.7279	5772.2815	5772.8324
		NAT	6264.6763	5771.7275	5772.2807	5772.8338

Table 12 The first five natural frequencies of the free-clamped Timoshenko beam with three changes in cross-sections and carrying three lumped mass and/or three rotary inertias for different values of N_r

Attachments m_n , $I_{0,s}$ (n=s=1, 2, 3)	ω_α (rad/sec)	METHOD	(BEBT) N_r=0.00	(TBT) N_r=0.00	(TBT) N_r=0.10	(TBT) N_r=0.20
m_n	ω_1	DTM $(\bar{N}=42)$	363.6915	359.9651	360.8453	361.7224
		NAT	363.6915	359.9651	360.8453	361.7221
	ω_2	DTM $(\bar{N}=48)$	1163.4392	1134.2011	1135.5040	1136.8068
		NAT	1163.4392	1134.2011	1135.5048	1136.8061
	ω_3	DTM $(\bar{N}=54)$	2475.7427	2299.7289	2300.6600	2301.5925
		NAT	2475.7426	2299.7284	2300.6597	2301.5911
	ω_4	DTM $(\bar{N}=60)$	5309.9510	4769.6919	4770.1627	4770.6339
		NAT	5309.9511	4769.6918	4770.1621	4770.6323
	ω_5	DTM $(\bar{N}=68)$	8287.2256	6254.2770	6254.6019	6254.9258
		NAT	8287.2252	6254.2775	6254.6012	6254.9247
m_n , $I_{0,s}$	ω_1	DTM $(\bar{N}=42)$	354.2023	350.9590	351.7977	352.6330
		NAT	354.2023	350.9588	351.7981	352.6338
	ω_2	DTM $(\bar{N}=48)$	1107.5328	1081.4575	1082.5648	1083.6685
		NAT	1107.5324	1081.4581	1082.5640	1083.6674
	ω_3	DTM $(\bar{N}=54)$	2178.5565	2102.0149	2103.0623	2104.1108
		NAT	2178.5562	2102.0143	2103.0620	2104.1099
	ω_4	DTM $(\bar{N}=60)$	3449.9718	3251.7054	3252.1549	3252.6048
		NAT	3449.9718	3251.7049	3252.1543	3252.6040
	ω_5	DTM $(\bar{N}=68)$	6328.3044	5597.5224	5598.0364	5598.5523
		NAT	6328.3042	5597.5229	5598.0372	5598.5514

6. Conclusions

In this study, the frequency values and the mode shapes for free vibration of the axial-loaded Timoshenko multiple-step beam carrying a number of intermediate lumped masses and/or rotary inertias are investigated by using DTM and NAT. In three numerical examples, the frequency values are determined for Timoshenko beams with/without the axial force effect and these values are presented in the tables. The frequency values obtained for the Timoshenko beams without the axial force effect are less than the values obtained for the Bernoulli-Euler beams, as expected, since the shear deformation is considered in Timoshenko beam theory. The increase in the values of axial force also causes an increase in the frequency values for three different boundary conditions.

It can be seen from the tables that the frequency values show a very high decrease as a lumped mass is attached to the beam. The rotary inertias have significant influence on the first five natural frequencies of the axial-loaded Timoshenko multiple-step beam with pinned-pinned, clamped-free and free-clamped boundary conditions. The first five natural frequencies and the associated mode shapes of the pinned-pinned, clamped-free and free-clamped Timoshenko beam carrying a number of lumped masses together with their rotary inertias are different from the corresponding ones of the same beam carrying the same lumped masses only for N_r is being constant.

The essential steps of the DTM application includes transforming the governing equations of motion into algebraic equations, solving the transformed equations and then applying a process of inverse transformation to obtain any desired natural frequency. All the steps of the DTM are very straightforward and the application of the DTM to both the equations of motion and the boundary conditions seem to be very involved computationally. However, all the algebraic calculations are finished quickly using symbolic computational software. Besides all these, the analysis of the convergence of the results show that DTM solutions converge fast. When the results of the DTM are compared with the results of NAT, very good agreement is observed.

References

Chen, D.W. and Wu, J.S. (2002), “The exact solutions for the natural frequencies and mode shapes of non-uniform beams with multiple spring-mass system”, *J. Sound Vib.*, **255**, 299-322.

Chen, D.W. (2003), “The exact solutions for the natural frequencies and mode shapes of non-uniform beams carrying multiple various concentrated elements”, *Struct. Eng. Mech.*, **16**, 153-176.

Çatal, S. (2006), “Analysis of free vibration of beam on elastic soil using differential transform method”, *Struct. Eng. Mech.*, **24**(1), 51-62.

Çatal, S. and Çatal, H.H. (2006), “Buckling analysis of partially embedded pile in elastic soil using differential transform method”, *Struct. Eng. Mech.*, **24**(2), 247-268.

Çatal, S. (2008), “Solution of free vibration equations of beam on elastic soil by using differential transform method”, *Appl. Math. Model.*, **32**, 1744-1757.

Çatal, S. (2012), “Response of forced Euler-Bernoulli beams using differential transform method”, *Struct. Eng. Mech.*, **42**, 95-119.

Gürgöze, M. (1984), “A note on the vibrations of restrained beams and rods with point masses”, *J. Sound Vib.*, **96**, 461-468.

Gürgöze, M. (1985), “On the vibration of restrained beams and rods with heavy masses”, *J. Sound Vib.*, **100**, 588-589.

Gürgöze, M. and Batan, H. (1996), “On the effect of an attached spring-mass system on the frequency spectrum of a cantilever beam”, *J. Sound Vib.*, **195**, 163-168.

Gürgöze, M. (1996), "On the eigenfrequencies of a cantilever beam with attached tip mass and a spring-mass system", *J. Sound Vib.*, **190**, 149-162.

Gürgöze, M. (1998), "On the alternative formulation of the frequency equation of a Bernoulli-Euler beam to which several spring-mass systems are attached in-span", *J. Sound Vib.*, **217**, 585-595.

Gürgöze, M. and Erol, H. (2001), "Determination of the frequency response function of a cantilever beam simply supported in-span", *J. Sound Vib.*, **247**, 372-378.

Gürgöze, M. and Erol, H. (2002), "On the frequency response function of a damped cantilever beam simply supported in-span and carrying a tip mass", *J. Sound Vib.*, **255**, 489-500.

Hamdan, M.N. and Jubran, B.A. (1991), "Free and forced vibrations of a restrained uniform beam carrying an intermediate lumped mass and a rotary inertia", *J. Sound Vib.*, **150**, 203-216.

Jaworski, J.W. and Dowell, E.H. (2008), "Free vibration of a cantilevered beam with multiple steps: Comparison of several theoretical methods with experiment", *J. Sound Vib.*, **312**, 713-725.

Ju, F., Lee, H. P. and Lee, K. H. (1994), "On the free vibration of stepped beams", *Int. J. Solid. Struct.*, **31**, 3125-3137.

Kaya, M.O. and Ozgumus, O.O. (2007), "Flexural-torsional-coupled vibration analysis of axially loaded closed-section composite Timoshenko beam by using DTM", *J. Sound Vib.*, **306**, 495-506.

Koplow, M.A., Bhattacharyya, A. and Mann, B.P. (2006), "Closed form solutions for the dynamic response of Euler-Bernoulli beams with step changes in cross-section", *J. Sound Vib.*, **295**, 214-225.

Lin, H.P. and Chang, S.C. (2005), "Free vibration analysis of multi-span beams with intermediate flexible constraints", *J. Sound Vib.*, **281**, 155-169.

Lin, H.Y. and Tsai, Y.C. (2005), "On the natural frequencies and mode shapes of a uniform multi-span beam carrying multiple point masses", *Struct. Eng. Mech.*, **21**, 351-367.

Lin, H.Y. and Tsai, Y.C. (2006), "On the natural frequencies and mode shapes of a multiple-step beam carrying a number of intermediate lumped masses and rotary inertias", *Struct. Eng. Mech.*, **22**, 701-717.

Lin, H.Y. and Tsai, Y.C. (2007), "Free vibration analysis of a uniform multi-span beam carrying multiple spring-mass systems", *J. Sound Vib.*, **302**, 442-456.

Lin, H.Y. (2008), "Dynamic analysis of a multi-span uniform beam carrying a number of various concentrated elements", *J. Sound Vib.*, **309**, 262-275.

Lin, H.Y. (2010), "An exact solution for free vibrations of a non-uniform beam carrying multiple elastic-supported rigid bars", *Struct. Eng. Mech.*, **34**, 399-416.

Liu, W.H., Wu, J.R. and Huang, C.C. (1998), "Free vibration of beams with elastically restrained edges and intermediate concentrated masses", *J. Sound Vib.*, **122**, 193-207.

Naguleswaran, S. (2002a), "Natural frequencies, sensitivity and mode shape details of an Euler-Bernoulli beam with one-step change in cross-section and with ends on classical supports", *J. Sound Vib.*, **252**, 751-767.

Naguleswaran, S. (2002b), "Vibration of an Euler-Bernoulli beam on elastic end supports and with up to three-step changes in cross-section", *Int. J. Mech. Sci.*, **44**, 2541-2555.

Naguleswaran, S. (2002c), "Transverse vibrations of an Euler-Bernoulli uniform beam carrying several particles", *Int. J. Mech. Sci.*, **44**, 2463-2478.

Naguleswaran, S. (2003a), "Transverse vibration of an Euler-Bernoulli uniform beam on up o five resilient supports including ends", *J. Sound Vib.*, **261**, 372-384.

Naguleswaran, S. (2003b), "Vibration and stability of an Euler-Bernoulli beam with up to three-step changes in cross-section and in axial force", *Int. J. Mech. Sci.*, **45**, 1563-1579.

Naguleswaran, S. (2004a), "Transverse vibration and stability of an Euler-Bernoulli beam with step change in cross-section and in axial force", *J. Sound Vib.*, **270**, 1045-1055.

Naguleswaran, S. (2004b), "Vibration of an Euler-Bernoulli stepped beam carrying a non-symmetrical rigid body at the step", *J. Sound Vib.*, **271**, 1121-1132.

Ozgumus, O.O. and Kaya, M.O. (2007), "Energy expressions and free vibration analysis of a rotating double tapered Timoshenko beam featuring bending-torsion coupling", *Int. J. Eng. Sci.*, **45**, 562-586.

Ozgumus, O.O. and Kaya, M.O. (2006), "Flapwise bending vibration analysis of double tapered rotating Euler-Bernoulli beam by using the differential transform method", *Meccanica*, **41**, 661-670.

Özdemir, Ö. and Kaya, M.O. (2006), “Flapwise bending vibration analysis of a rotating tapered cantilever Bernoulli-Euler beam by differential transform method”, *J. Sound Vib.*, **289**, 413-420.

Wang, J.R., Liu, T.L. and Chen, D.W. (2007), “Free vibration analysis of a Timoshenko beam carrying multiple spring-mass systems with the effects of shear deformation and rotatory inertia”, *Struct. Eng. Mech.*, **26**, 1-14.

Wu, J.S. and Chou, H.M. (1999), “A new approach for determining the natural frequencies and mode shape of a uniform beam carrying any number of spring masses”, *J. Sound Vib.*, **220**, 451-468.

Wu, J.S. and Chen, D.W. (2001), “Free vibration analysis of a Timoshenko beam carrying multiple spring-mass systems by using the numerical assembly technique”, *Int. J. Numer. Meth. Eng.*, **50**, 1039-1058.

Wu, J.S. and Chang, B.H. (2013), “Free vibration of axial-loaded multi-step Timoshenko beam carrying arbitrary concentrated elements using continuous-mass transfer matrix method”, *Euro. J. Mech. A/Solid.*, **38**, 20-37.

Yesilce, Y., Demirdag, O. and Catal, S. (2008), “Free vibrations of a multi-span Timoshenko beam carrying multiple spring-mass systems”, *Sadhana*, **33**, 385-401.

Yesilce, Y. and Demirdag, O. (2008), “Effect of axial force on free vibration of Timoshenko multi-span beam carrying multiple spring-mass systems”, *Int. J. Mech. Sci.*, **50**, 995-1003.

Yesilce, Y. and Catal, S. (2009), “Free vibration of axially loaded Reddy-Bickford beam on elastic soil using the differential transform method”, *Struct. Eng. Mech.*, **31**(4), 453-476.

Yesilce, Y. (2010), “Effect of axial force on the free vibration of Reddy-Bickford multi-span beam carrying multiple spring-mass systems”, *J. Vib. Control*, **16,** 11-32.

Zhou, J.K. (1986), *Differential transformation and its applications for electrical circuits*, Huazhong University Press, Wuhan China.

CC

Appendix

The details for the application of Hamilton's principle and the derivation of the equations of motion are presented below.

The virtual kinetic energy δV_i and the virtual potential energy $\delta \Pi_i$ can be written for i^{th} segment of an axial-loaded Timoshenko multiple-step beam as

$$\delta V_i = \int_0^{L_i} \left[\overline{m}_i \cdot \frac{\partial y_i(x_i,t)}{\partial t} \cdot \frac{\partial \delta y_i(x_i,t)}{\partial t} + \frac{\overline{m}_i \cdot I_i}{A_i} \cdot \frac{\partial \phi_i(x_i,t)}{\partial t} \cdot \frac{\partial \delta \phi_i(x_i,t)}{\partial t} \right] \cdot dx_i \tag{A.1}$$

$$\begin{aligned} \delta \Pi_i = & \int_0^{L_i} \left[EI_i \cdot \frac{\partial \phi_i(x_i,t)}{\partial x_i} \cdot \frac{\partial \delta \phi_i(x_i,t)}{\partial x_i} \right] \cdot dx_i \\ & + \int_0^{L_i} \left[\frac{GA_i}{\overline{k}} \cdot \left(\frac{\partial y_i(x_i,t)}{\partial x_i} - \phi(x_i,t) \right) \cdot \left(\frac{\partial \delta y_i(x_i,t)}{\partial x_i} - \delta\phi(x_i,t) \right) - N \frac{\partial y_i(x,t)}{\partial x_i} \cdot \frac{\partial \delta y_i(x_i,t)}{\partial x_i} \right] \cdot dx_i \\ & (i = 1, 2, ..., h+1) \end{aligned} \tag{A.2}$$

The equations of motion for an axial-loaded Timoshenko multiple-step beam are derived by applying Hamilton's principle, which is given by

$$\delta \int_{t_1}^{t_2} \int_0^{L_i} L_{g,i} \cdot dx_i \cdot dt = 0 \tag{A.3}$$

where

$$L_{g,i} = V_i - \Pi_i \tag{A.4}$$

is termed as the Lagrangian density function.

By taking the variation of the Lagrangian density function; integrating Eq. (A.3) by parts, and then collecting all the terms of the integrand with respect to $\delta y_i(x_i,t)$ and $\delta\theta_i(x_i,t)$, one can derive the following equations of motion as the coefficients of $\delta y_i(x_i,t)$ and $\delta\theta_i(x_i,t)$

$$EI_i \cdot \frac{\partial^2 \phi_i(x_i,t)}{\partial x_i^2} + \frac{GA_i \cdot}{\overline{k}} \cdot \left(\frac{\partial y_i(x_i,t)}{\partial x_i} - \phi_i(x_i,t) \right) - \frac{\overline{m}_i \cdot I_i}{A_i} \cdot \frac{\partial^2 \phi_i(x_i,t)}{\partial t^2} = 0 \tag{A.5}$$

$$\frac{GA_i \cdot}{\overline{k}} \cdot \left(\frac{\partial^2 y_i(x_i,t)}{\partial x_i^2} - \frac{\partial \phi_i(x_i,t)}{\partial x_i} \right) - N \cdot \frac{\partial^2 y_i(x_i,t)}{\partial x_i^2} - \overline{m}_i \cdot \frac{\partial^2 y_i(x_i,t)}{\partial t^2} = 0 \tag{A.6}$$